

**The apportionment of tooth size and its implications in *Australopithecus sediba* versus other Plio-Pleistocene and recent African hominins**

Joel D. Irish<sup>1,4,\*</sup>, Brian E. Hemphill<sup>2</sup>, Darryl J. de Ruiter<sup>3,4</sup>, and Lee R. Berger<sup>4</sup>

1. Research Centre in Evolutionary Anthropology and Palaeoecology, School of Natural Sciences and Psychology, Liverpool John Moores University, Liverpool L3 3AF UK.
2. Department of Anthropology, University of Alaska, Fairbanks, AK 99775 USA.
3. Department of Anthropology, Texas A&M University, College Station, TX 77843 USA.
4. Evolutionary Studies Institute and Centre for Excellence in PaleoSciences, University of the Witwatersrand, Private Bag 3, WITS 2050, Johannesburg, South Africa.

23 text pages  
12 reference pages  
1 footnote page  
8 tables  
10 figures

Running Title: *Australopithecus sediba* odontometrics

**KEY WORDS** Odontometrics, geometric means, principal components analysis, phenetic affinities

Send correspondence to: Prof. Joel D. Irish, Research Centre in Evolutionary Anthropology and Palaeoecology, School of Natural Sciences and Psychology, Liverpool John Moores University, Byrom Street, Liverpool, L3 3AF, United Kingdom +44 (0)151 231 2387 (Office)  
+44 (0)151 231 2338 (Fax)  
[J.D.Irish@ljmu.ac.uk](mailto:J.D.Irish@ljmu.ac.uk)

Grant sponsors: National Science Foundation (BCS-0840674, BNS-9013942) to JDI; Council for the International Exchange of Scholars to BEH; Texas A&M University Ray A. Rothrock Fellowship, Cornerstone Faculty Fellowship, and College of Liberal Arts Seed Program to DJD.

## ABSTRACT

**Objectives:** *Australopithecus sediba* is characterized further by providing formerly unpublished and refined mesiodistal and buccolingual crown measurements in the MH1 and MH2 specimens. After size correction, these data were compared with those in other fossil and recent samples to facilitate additional insight into diachronic hominin affinities.

**Materials and Methods:** Six comparative samples consist of fossil species: *A. africanus*, *A. afarensis*, *Homo habilis*, *Paranthropus robustus*, *P. boisei*, and *H. erectus*. Others comprise *H. sapiens* and *Pan troglodytes*. Re-estimates of “actual” dimensions in damaged *A. sediba* teeth were effected through repeated measurements by independent observers. X-ray synchrotron microtomography allowed measurement of crowns obscured by matrix and non-eruption. Tooth size apportionment analysis, an established technique for intraspecific comparisons, was then applied at this interspecific level to assess phenetic affinities using both within- and among-group data.

**Results:** Comparison of these highly heritable dimensions identified a general trend for smaller posterior relative to larger anterior teeth (not including canines), contra *Paranthropus*, that allies *A. sediba* with other australopiths and *Homo*; however, specific reductions and/or shape variation in the species’ canines, third premolars, and anterior molars relative to the other teeth mirror the patterning characteristic of *Homo*.

**Discussion:** Of all samples, including east African australopiths, *A. sediba* appears most like *H. habilis*, *H. erectus* and *H. sapiens* regarding how crown size is apportioned along the tooth rows. These findings parallel those in prior studies of dental and other skeletal data, including several that suggest *A. sediba* is a close relative of, if not ancestral to, *Homo*.

The dental morphology of *Australopithecus sediba* has been characterized and compared with that of various fossil and recent hominins (Berger et al., 2010; de Ruiter et al., 2013; Irish et al., 2013, 2014). Dental measurements were also presented (Berger et al., 2010; de Ruiter et al., 2013) though, with exception (de Ruiter et al., 2013), inter-sample study of crown dimensions has been more limited. In brief, these earlier studies suggested the species: 1) is distinct from east African australopiths, 2) may be a sister species of *A. africanus*, and 3) along with *A. africanus*, is positioned at the stem of a clade comprising *Homo*, or otherwise shares a close relationship with the latter genus (i.e., Dembo et al., 2015). Dental morphological apomorphies relative to earlier australopiths, as well as *Gorilla* and *Pan*, include: faint shoveling of the upper central incisors (UI1), size variation between the two lingual cusps of lower fourth premolars (LP4), and increased expressions of key upper and lower molar variants (Carabelli's UM1, protostylid LM1, cusp 7 LM1) (Berger et al., 2010; Irish et al., 2013, 2014). Odontometric apomorphies include general size reduction and a specific decrease in the canines and several posterior teeth, like that seen in later *Homo* (Berger et al., 2010; de Ruiter et al., 2013).

The objective of this report is to expand further upon the latter topic, i.e., odontometrics in *A. sediba* and interspecific relationships. First, previously unpublished and several revised mesiodistal (MD) and buccolingual (BL) measurements are presented in the 1.977 Ma year-old MH1 Holotype and MH2 Paratype. The diameters are revised, albeit minimally, in that they are based on repeated-measures (re)estimates of worn and fractured crowns, and x-ray synchrotron microtomographic scans of teeth that were unerupted or are covered by matrix. Published data of the latter had originally been taken from lower resolution medical CT scans. Second, the highly heritable MD and BL crown dimensions (Alvesalo and Tigerstedt, 1974; Townsend and Brown, 1980; Kieser, 1990; Dempsey et al., 1995; Dempsey and Townsend, 2001; Hlusko et al., 2002;

Townsend et al., 2003; Baydas et al., 2005; Rizk et al., 2008), where in some studies  $h^2 > 0.8$  (e.g., Dempsey and Townsend, 2001), are used to compare *A. sediba* with samples of eight other species: *A. africanus*, *A. afarensis*, *Homo habilis*, *Paranthropus robustus*, *P. boisei*, *H. erectus* (*ergaster*), recent *H. sapiens*, and *Pan troglodytes*. To do so, a proven method known as tooth size apportionment (TSA) analysis is employed to identify among-sample phenetic affinities.

Like all skeletal measurements, odontometric data may be divided into two components for analysis: (absolute) size and shape (relative size) (Penrose, 1954; Rahman, 1962; Corruccini, 1973; Smith, 1981b; Wolpoff, 1985; Harris and Harris, 2007; Brook et al., 2008; Suwa et al., 2009; Townsend et al., 2009). Both components are useful, depending on the question(s) being asked. However, in the present study significant differences between small- (e.g., *H. sapiens*, *Pan troglodytes*) and large-toothed (*P. boisei*, *P. robustus*) samples are such that the interspecific variation will be disproportionately influenced by size differences alone (as demonstrated by Corruccini, 1973, and below; also see Penrose, 1954; Rahman, 1962; Mayer, 1969; Harris and Bailit, 1988, Harris and Rathbun, 1991; Harris and Harris, 2007; Townsend et al., 2009). Such differences may or may not be allometrically equivalent (e.g., Gould, 1975; Felsenstein, 1985; Gingerich and Smith, 1985; Pagel and Harvey, 1988, 1989; Harvey et al., 1991; Copes and Schwartz, 2010) and might be affected by differing levels and patterns of sex dimorphism, life history factors, diet, and/or social group structure (Gingerich and Schoeninger, 1979; Smith 1981a; Kay et al., 1988; Kieser, 1990; Leigh, 1992; Plavcan, 2001; Toma et al., 2007; Pilloud et al., 2014). Thus, the crown measurements were mathematically corrected so that all samples are equivalently scaled (among all teeth within dentitions) using an approach termed DM\_RAW (from Jungers et al., 1995; after Darroch and Mosimann, 1985). Though not directly evaluated, it follows that the heritability of these scaled data is comparable to that of the original MD and BL

dimensions (above), as all measurements before and after correction (see Results) are highly correlated ( $r=0.94$ ,  $p=0.00$ ).

The among-sample scaled dimensions were then used in the TSA analysis to examine the distribution, or patterning, of relative crown size along the tooth rows by sample (Harris, 1997, 1998). To date, this method has been used exclusively to characterize and compare samples of recent humans, i.e., within species (Harris and Bailit, 1988; Harris and Rathbun, 1991; Hemphill et al., 1992; Lukacs and Hemphill, 1993; Harris, 1997, 1998; Irish and Hemphill, 2001; Irish and Kenyhercz, 2013). Here, TSA is applied to do the same among species of hominins and *Pan* that differ markedly in apportionment of tooth size relative to humans. Various imaging methods are available that can quantify such variation (Kato and Ohno, 2009; Mitteroecker and Gunz, 2009; Baab et al., 2012; Braga, 2016; Hemphill, 2016a); yet, they are time intensive and the heritability of phenotype captured is comparable to that derived from basic linear estimates (e.g., Hlusko et al., 2002 and below). Thus, the phenetic affinity of *A. sediba* to the other species is considered using two basic, readily obtainable measurements of the permanent teeth.

## **METHODS**

Maximum crown dimensions were recorded in each of the total 29 teeth from the juvenile MH1 male and adult MH2 female (Berger et al., 2010) following the standard, established protocol (Moorrees and Reed, 1964) used by odontometricians in all subfields of biological anthropology, including paleoanthropology: the MD dimension is measured parallel to the occlusal and labial/buccal surfaces, whereas the BL is measured as the greatest distance perpendicular to the MD (Hemphill, 2016a). Measurements were taken with needle point calipers accurate to 0.05 mm.

Re-estimates of “actual” biological diameters for worn and damaged crowns permitted refinement of several measurements. Where hindered by remnant matrix and non-eruption (see

Berger et al., 2010; de Ruiter et al., 2013; Irish et al., 2013), dimensions were estimated from medical CT scans for the original 2010 *A. sediba* study (Berger et al., 2010). Subsequently, propagation phase contrast x-ray synchrotron microtomography was undertaken, from which more precise measurements could be taken for the present study. Scanning was performed at the European Synchrotron Radiation Facility, in Grenoble, France. For the mandible scan, the ID19 beamline was used with a propagation distance of 900 mm and a polychromatic beam. The wiggler source was set at a gap of 73 mm, filtered with 3 mm of aluminum and 1 mm of Cu, and coupled with a scintillator screen in gadox 25 microns thick. The resulting average detected energy was 62.3 keV. Each sub-scan was done in half-acquisition mode (double lateral field of view), using 5,000 projections of 0.2s each with a FReLoN CCD camera in frame transfer mode. The sample was moved vertically by 4.5 mm between each scan. All of the reconstructions were performed using a single distance phase retrieval algorithm. Slices were then corrected for ring artifacts, and all the sub-scans were concatenated together to generate a single scan of the whole specimen (Tafforeau, pers. comm. 2015). For the maxillary dentition, the ID17 beamline was used. The protocol is detailed elsewhere (Carlson et al., 2011), but in brief, a beam of 5 x 96 mm in half-acquisition geometry was used to acquire projections of 1s each over 360 degrees of the specimen. From the original high resolution data (isotropic voxel size of 45.71  $\mu\text{m}$ , 50 Gb in 16 bits), a lower resolution data set was generated (91.42  $\mu\text{m}$ , 6.4 Gb in 16 bits) for easier data handling. To distinguish bone/teeth from matrix, lower (18000) and upper thresholds (31000) were used for segmentation. Supplementary image processing (for removal of additional matrix) was done with Avizo 6.3 and VGStudio MAX 2.1 before transferring the calculated mask back to the full resolution data set (Carlson et al., 2011).

Two authors, JDI and DJD, independently took repeated MD and BL measurements of each MH1 and MH2 crown. No significant intra-observer error was detected. Measurements of both observers were then compared, for which there also was no significant difference (paired-samples t-test,  $p < 0.05$ ). For slight variations the mean dimension was calculated on the basis that random errors tend to be normally distributed about the true measure (Hemphill, 2016a). Those dimensions (refer to Table 1) that do vary from the originals do so minimally, and no significant differences were detected. The comparability of MD and BL crown measurements taken with calipers vs. those from CT scans has not been specifically tested, although enamel thickness has been [i.e., micro focal X-ray computed tomography (e.g., Olejniczaki and Grine, 2006)]; these results ranged from excellent to poor equivalency – in the case of thin enamel (i.e.,  $< 0.10$  mm). Given the larger scale of crown size and much higher resolution of synchrotron scans relative to this enamel thickness study, any inter-method error should be minimal. Measurement landmarks are the same and the accuracy of the calipers is approximately equivalent to that of the scan data (Carlson, pers. comm., 2016).

For the comparative analyses, any redundancy between right and left antimeres was avoided by using mean MD and BL data in both specimens where the tooth pairs are retained; if only the right or left tooth of an antimeric pair is present, its dimensions were used to reach 16 possible measurements in each isomere.

Tooth size apportionment analysis (TSA) was employed to compare species. The unit of study is the dentition as a whole, i.e., how crown size varies within it, instead of focusing on the individual tooth dimensions (Harris and Bailit, 1988; Harris and Rathbun, 1991; Hemphill et al., 1992; Lukacs and Hemphill, 1993; Harris, 1997, 1998; Irish and Hemphill, 2001). In prior study of recent humans, TSA has been conducted at two levels: within-group (a.k.a., inter-individual)

and among-group. At the former level, a correlation matrix of tooth measurements in a sample of individuals with complete dentitions from one population is submitted to principal components analysis (PCA). At the among-group level a correlation matrix of mean MD and BL data from multiple samples is submitted to PCA. The resulting uncorrelated components are then used to facilitate comparisons among samples based on patterns of intertooth relationships. Here, the goal is to compare patterning among hominin species; to do so, a modified approach of Harris and others is followed (Harris and Bailit, 1988; Harris and Rathbun, 1991; Hemphill et al., 1992; Lukacs and Hemphill, 1993; Harris, 1997, 1998; Irish and Hemphill, 2001; Hemphill, 2016b).

Ordinarily, to minimize the size effects that dominate component 1 in TSA analyses of recent humans, residual scores are calculated and substituted (Harris, 1997). However (as above), size correction is critical here given the significant differences among hominin species. Thus, an alternate method advocated by Jungers et al. (1995). i.e., the DM\_RAW correction (Darroch and Mosimann, 1985), was used (also Irish and Kenyhercz, 2013). Specifically, the geometric mean (GM) is computed as the  $n$ th root of the product for all  $n$  measurements ( $x$ ) per case. Each of the measurements is then divided by this mean ( $x/GM$ ) for that case to yield an average value of 1.0 across rows. Such scaling effectively “cancels out size differences by giving each individual [or sample] the same average character state or magnitude over all the measurements taken on it” (Corruccini, 1973, p 747). Once calculated, the correlation matrix of DM\_RAW-corrected mean MD and BL diameters was submitted to PCA to obtain component loadings, with the resulting group component scores plotted in three dimensions to help visualize interspecific variation. All statistical analyses were performed using SPSS (Ver. 21.0).

Maxillary and mandibular teeth are generally analyzed simultaneously to produce the maximum characterization and differentiation in apportionment of tooth size. However, the



missing measurements in *A. sediba* (refer to Table 1) prompted initial separate comparisons with the other hominin and *Pan* samples: maxillary teeth only with data from MH1, and mandibular teeth using measurements from MH2. In both cases, within-group data (*A. sediba*) are compared directly to among-group data (all other species). Correlation matrices from these alternate data are strongly correlated (e.g.,  $r=0.70$ ). Still, to address potential data incompatibility the simplest strategy is to assume that MH1 and MH2, each with a sample size of  $n=1$  for the maxillary and mandibular comparisons, are representative of *A. sediba*. Doing so provides compatibility in the among-group data analysis across comparative samples, while at least permitting some indication of *A. sediba*'s phenetic affinity to the other species.

A second strategy is to undertake a comparison at the level of the individual. However, the requisite complete fossil dentitions are not available. What is required is the construction of samples drawn from modern humans, with complete dentitions, that parallel the characteristics of the fossil hominin dental assemblages. Measurements of four modern samples are used here (see Materials). Unfortunately, sampling protocols that specifically targeted young adults having minimally worn teeth means that the overwhelming majority of individuals lacked third molars. For this reason, all third molars were excluded from consideration in this phase of the analysis. Thus, with this exception, a series of random samples were drawn from each modern sample that mimic as closely as possible the number of individuals and representation by dental element of the average fossil taxon. The latter information was obtained by averaging the fossil comparative samples by taxon, dental element, and number of individuals. All crown diameters captured in each of these sampling events were then averaged to obtain a "meta-individual," in which each measurement was subsequently size-corrected, i.e., geometrically scaled. The same process was repeated until the number of meta-individuals was the same as that for the average fossil taxon.

Next, comparative fossil samples were resampled in the same manner; *Pan* was excluded. The meta-individuals, i.e., replicates, provide the unit of analysis for TSA comparison with *A. sediba*, i.e., here with data from MH1 and MH2 combined. Therefore, separate maxillary and mandibular analyses are unnecessary because these teeth are compared simultaneously.

## MATERIALS

Ongoing fossil recovery has led to an ability to analyze samples, some of which are more representative than others, to help quantify intraspecific variation for interspecific comparisons. Of the current comparative samples, six consist of African Plio-Pleistocene species based on directly-recorded (by DJD) or published data (see Robinson, 1956; Tobias, 1967, 1991; Wolpoff, 1971; Johanson et al., 1982; Grine, 1989; Wood, 1991; Grine and Daegling, 1993; Grine and Strait, 1994; Gabunia and Vekua, 1995; Kimbel et al., 1997; de Ruiter, 2004; Kimbel et al., 2004; Moggi-Cecchi et al., 2006; White et al., 2006; Suwa et al., 2007; Martínón-Torres et al., 2008; Lordkipanidze et al., 2013; Berger et al., 2015). In the latter cases, where reported, the measurement technique was identified for conformity with the above protocol (Moorrees and Reed, 1964) to promote data compatibility; of course, inter-observer error could not be assessed.

The fossil samples were selected because they: 1) originate in the two primary hominin geographic regions of Africa, i.e., east and south, 2) represent three key later Plio-Pleistocene genera and, most simply, 3) are the only African species with multiple measurements for all permanent teeth. They are: *A. africanus* (307 total teeth), *A. afarensis* (271 teeth), *Paranthropus robustus* (377 teeth), *P. boisei* (172 teeth), *H. habilis* (93 teeth), and *H. erectus* (260 teeth). The very few anterior teeth recovered from the latter species in Africa necessitated supplementation, so data from 38 crowns in what is identified as *H. erectus ergaster* (or at least a close relative of

similar age) from Dmanisi (Rightmire et al., 2006; Baab, 2008; Martínón-Torres et al., 2008; Rightmire and Lordkipanidze, 2010; Lordkipanidze et al., 2013) are also included.

For the separate maxillary and mandibular among-group TSA comparisons, one sample (>8,300 total teeth;  $n=822$  individuals) of *H. sapiens* is included that consists of measurements taken (by JDI) in post-Pleistocene sub-Saharan Africans. A non-hominin *Pan troglodytes* (924 teeth;  $n=70$  individuals) sample is included to help demonstrate methodological effectiveness, while emphasizing among-species taxonomic variation (Mahler, 1973). For TSA within-group analysis of the meta-individuals, *H. sapiens* is represented by four dental cast samples of modern people. Initially, South African San (>1,100 teeth;  $n=83$ ) and Pedi (or Northern Sotho) (>2,400 teeth;  $n=177$ ) were considered (Haeussler et al., 1989; Irish, 1993); however, to move beyond local population-level variation, i.e., promote taxonomic variability, two Indian samples of Bhils (>2,800 teeth;  $n=208$ ) and Garasias (>2,800 teeth;  $n=207$ ) (Lukacs and Hemphill, 1993) were included. In these instances sample selections were based on availability as well as, critically, dental completeness (with exceptions noted).

Ideally, analyses would be conducted separately by sex, although this strategy was not followed in the earlier TSA analyses. In recent humans tooth size is not allometrically scaled to a significant degree, so males and females from the same population will differ in absolute size but relative tooth size apportionment is unaffected by sexual dimorphism (Harris and Rathbun, 1991; Hemphill et al., 1992; Hemphill, 2016b). The same cannot be assumed for the fossil species with, for example, greater body size differences between the sexes. Nevertheless, at least in recent humans, dimorphism is mainly (80%) a matter of ontogenetic scaling, so the pattern of tooth size variation among species should not be substantially altered (Hemphill, 2016b); this is especially true for the within-group analysis, where all measurements were geometrically scaled for each

meta-individual. In any event, it is out of necessity, including an inability to assign sex to most fossil specimens, many missing data, and a need to maximize the already-small sample sizes, that the sexes be pooled by species.

## RESULTS

The odontometric measurements of *A. sediba* are presented in Table 1. Many dimensions could not be recorded, though among the 29 teeth in the right and left dental arches of MH1 and MH2, most MD and BL diameters of the 32 permanent teeth are listed at least once; the exceptions are the MD dimensions of the lower first (LI1) and second incisors (LI2), because both teeth are too worn to attempt visual approximation. A total of 36 measurements from the original study (i.e., Berger et al., 2010) were either revised, albeit insignificantly (above) between 0.1 to 1.0 mm, or are presented for the first time in the case of MH1 right maxillary postcanine teeth (Fig. 1). Mean odontometric data for the relevant comparative samples are listed in Table 2.

**[TABLES 1-2 and FIGURE 1 HERE]**

### **The MH1 Maxillary Dentition Comparison**

The MH1 occlusal surface areas (MD x BL) were first calculated by tooth for comparison with the other sample data. These products provide rough estimates of actual crown areas (Garn et al., 1977; Hemphill, 2016a). Nonetheless, they are useful as general indicators of dentition size (Hemphill, 2016a) and, as above, estimated and actual areas share the same heritability ( $h^2 = 0.83$ ), at least for the molars of close relatives (Hlusko et al., 2002). As evident in a line plot of tooth-by-tooth areas (Fig. 2), MH1 is intermediate in size compared to small- and large-toothed species. *Australopithecus sediba* trends the closest to *H. habilis* and *A. afarensis*, though the differential size reduction in certain teeth is evident (Berger et al., 2010) (as above). The MH1 canine (UC) is smaller than that in all comparative samples except the *Paranthropus* species and

*H. sapiens*; similarly, only *H. erectus* and *H. sapiens* have smaller upper third premolars (UP3) and second molars (UM2). This is not a cladistic study, but as mentioned the size of these teeth emulates the derived state present in later *Homo* species. Conversely, a more limited reduction of the upper fourth premolar (UP4) and perhaps upper third molar (UM3) relative to the adjacent UM2 in *A. sediba*, appears reminiscent of the condition in other australopiths and *H. habilis*.

**[FIGURE 2 HERE]**

Prior to the TSA analysis all 16 maxillary measurements were DM\_RAW size-corrected (Table 3). If these data are contrasted before and after correction it is evident how absolute tooth size is scaled among species. For instance, *P. boisei* and *H. sapiens* share the same mean UI1 BL size of 7.0 mm (Table 2); however, their respective corrected values are 0.61 and 0.82 (Table 3), which indicates that *P. boisei* has a smaller UI1 in this dimension relative to other teeth in the dentition. These species also share a corrected MD value of 1.22 for the upper first molar (UM1) (Table 3), but their respective absolute dimensions are 14.1 and 10.4 mm (Table 2).

**[TABLE 3 HERE]**

To demonstrate the effectiveness of DM\_RAW the data were submitted to hierarchical agglomerative cluster analysis before and after correction. A dendrogram can be produced to illustrate inter-sample phenetic relationships according to branching points in the display. Many algorithms are available but results from the average linkage (i.e., between groups) method are presented (Fig. 3). Each sample is initially considered as an individual cluster. The two most odontometrically-similar clusters, which may comprise one or more samples, are then joined based on the smallest average inter-sample distance between them. This process continues until one cluster results. Average linkage is the most common method (e.g., Everitt, 1980; Aldenderfer

and Blashfield, 1984; Romesburg, 1984), though the application of all seven available in SPSS (Ver. 21.0) (not shown) provides equivalent results, indicating stability of the solution.

**[FIGURE 3 HERE]**

Before (Fig. 3a), *H. sapiens* appears distinct from the other hominins, and closest to *Pan*. In a comparable odontometric experiment, Corruccini (1973 p 748) described these same “severe inconsistencies with accepted taxonomy” as being a “product of taxonomically unimportant size differences.” After size correction (Fig. 3b) the dendrogram appears similar to more generally accepted among-species relationships illustrated in cladograms from phylogenetic analyses. *Pan* is in a cluster of one. The two *Paranthropus* species again share a cluster, but now so do: 1) *H. erectus* and *H. sapiens*, and 2) *A. sediba* (MH1), *A. africanus*, *H. habilis*, and *A. afarensis*.

Although size-corrected these 32 total values remain inter-correlated, so they provide statistically redundant information (Corruccini, 1973; Harris, 1997). As such, for TSA analysis they were submitted to PCA to yield three uncorrelated components that account for 93.0% of the total variance. Each component’s loadings, their eigenvalues near or above 1.0, and variance explained are listed (Table 4). The group component scores are plotted in Figure 4. Together, this information can be used to characterize how tooth size is differentially apportioned or distributed within samples, and to compare variation in this patterning among samples.

**[TABLE 4 and FIGURE 4 HERE]**

Accounting for most of the variance (80.8%), component 1 identifies the major difference in size apportionment. *Paranthropus* possesses massive posterior relative to small anterior teeth. So strong loadings (i.e.,  $\geq |0.5|$ ) of 0.664 to 0.986 (Table 4) for relatively large, DM-corrected MD and BL dimensions of the UP3 to UM3 result in *P. boisei* and *P. robustus* being plotted near the positive end of the X axis in Figure 4, i.e., in this instance toward the top of plot.<sup>1</sup> On the

other hand, strongly negative (-0.831 to -0.966) loadings for DM\_MD and DM\_BL values in the UI1, upper lateral incisors (UI2), and UC push others, most notably *Pan* – with its spatulate incisors and prominent canines, toward the opposite end of the axis. The impetus for this sample distribution on the axis is apparent in Table 3. The *Paranthropus* species have the largest DM-corrected posterior tooth diameters of all samples, especially as compared to *Pan* which has the smallest. And, the reverse can be seen in the anterior teeth, as *Pan* has the largest DM-corrected anterior tooth diameters; *P. boisei* and *P. robustus* have the smallest. All others, including MH1, exhibit intermediate values (Table 3), which result in their locations near the center of the X axis.

Component 2 comprises 6.4% of the total variance. Samples are separated by size within the molar class. Specifically, the UM1 DM\_MD dimension has a strongly positive loading (0.546), while slightly less variation relates to DM\_BL (0.510); thus, the UM1 of high scorers on this axis is large compared to their adjacent UM2 and UM3. *Homo sapiens*, characterized by a size gradient of M1>M2>M3, is plotted toward the positive end of the Y axis; in Table 3 the UM1 DM\_MD and DM\_BL dimensions (1.22 and 1.31) are large relative to UM2 (1.16 and 1.32) and especially UM3 (1.04 and 1.29) contra most other samples, *A. africanus* in particular. The latter sample is nearest the negative end, where the UM1 DM\_MD (i.e., 1.16) and DM\_BL (1.25) size-corrected values (Table 3) are small relative to those of the UM2 (1.26 and 1.41) and UM3 (1.26 and 1.43). MH1 and *H. habilis*, at the center of the axis, share values of intermediate size, plus relatively long UM1s (below).

Component 3 accounts for 5.8% of the variance. There is just one strong loading and one of moderate magnitude in Table 4: again, the DM\_BL (loading of 0.521) and to a lesser extent the DM\_MD (-0.417) of UM1. High scorers on the Z axis, which include most samples, possess comparatively short DM\_MD and broad DM\_BL dimensions for this tooth, such as *A. afarensis*

(1.11 and 1.24, respectively in Table 3). The lowest scoring sample indicated in the figure, MH1, is characterized by relatively long DM\_MD (1.25) and narrow DM\_BL dimensions (1.19) for the UM1. Both of these corrected dimensions in nearby *H. habilis* are the same (i.e., 1.22; Table 3).

It was next decided to focus solely on similarities among the hominin samples, so *Pan* with its very distinct patterning of tooth size apportionment was dropped from analysis. Doing so produces some changes in the loadings, as evident when comparing Tables 4 and 5. Most notably both component 1 corrected-UM1 values (in Table 3) now play a minimal role in differentiating *Paranthropus* from the others (Table 5). On component 2, DM\_MDUI2 is much more important (with loading of 0.694) in driving variation, while the DM\_BLUM1 loading is less so (0.368). However, the total variance explained by the first three components (93.1%) is comparable, as is the sample distribution in a second plot (Fig. 5). The main differences are that the *Paranthropus* species appear more distant on the X axis, whereas MH1, *H. erectus* and, to a lesser extent, *H. habilis*, are nearer *H. sapiens* on the Y axis. Some variation in the latter grouping is driven by the sharing of long DM\_MDUI2 values relative to other samples (e.g., 0.70, 0.76, and .080 in MH1, *H. erectus*, and *H. sapiens*, respectively; Table 3), though not the extreme spatulate form in *Pan* (with DM\_MDUI2 corrected dimension of 0.86).

**[TABLE 5 and FIGURE 5 HERE]**

### **The MH2 Mandibular Dentition Comparison**

As noted, MD measurements of the LI1 and LI2 cannot be estimated due to heavy wear (Table 1; also see Fig. 7c below), so these data were deleted across all samples to leave just 14 DM\_RAW scaled measurements for TSA analysis (Table 3). Thus, in conjunction with estimated data for the worn posterior teeth, the results should be interpreted with caution relative to those from the MH1 maxillary dentition.



In absolute size the MH2 teeth are smaller than those in most samples but trend nearest *A. afarensis*, as illustrated in a second occlusal crown area plot (Fig. 6). Still, like the MH1 maxilla, the premolars, especially LP3, and molars (LM1, LM2, and LM3) are small, and the canine (LC) diminutive in comparison. Only *H. sapiens* has smaller estimated LC, LP3, and LP4 areas, and *H. erectus* and *H. sapiens* more reduced LM2s and LM3s. Again, differential decrease of these teeth in MH2 mirrors the arrangement in later *Homo*. Though much reduced, the relatively large LP4-to-LP3 and LM3-to-LM2 patterning is more like that present in *H. habilis* and the other australopiths – especially *A. africanus* (also compare *A. africanus*, *P. robustus*, MH2, *H. erectus*, and *H. sapiens* crown size variation in Fig. 7).

**[FIGURES 6-7 HERE]**

Regarding relative size, the first two components account for 90.2% of the total variance (see Table 6). The values for component 3 are also listed, but the small loadings, eigenvalue, and variance indicate little additional information; they are included because the group component scores are plotted in three dimensions (Fig. 8) to promote comparability among figures. Like the maxillary dentition, component 1 (81.5%) is dominated by strong positive loadings (i.e., 0.727-0.984) for relatively large posterior teeth, which again explains the location of *P. boisei* and *P. robustus* at the far end of the X axis. The key exception is the large negative loading (-0.853) for DM\_MDLP3; it relates to *Pan*'s sectorial LP3 (1.05 in Table 3) that, among other differences in relative size, helps to drive the sample toward the axis's near end. As above, all other samples are between these two extreme patterns. Lastly, on component 2 (7.7%) the UM1 of high scorers is, like the maxillary dentition, large compared to the adjacent UM2 and UM3. Thus, *H. sapiens* (UM1 DM\_MD and DM\_BL dimensions of 1.36 and 1.25 in Table 3) and to a lesser extent MH2

are near the positive end of the Y axis, whereas the *Paranthropus* and *Pan* samples plot toward the negative end.

**[TABLE 6 and FIGURE 8 HERE]**

After omitting *Pan*, *P. robustus* and *P. boisei* again plot near the positive end of the X axis for component 1 (61.2%) (Fig. 9 and Table 7), with relatively large posterior teeth other than LM1. Low scoring *Homo* and australopith samples have comparatively large anterior teeth. Component 2 (15.2%) separates *H. sapiens* on the basis of relatively large LM1s; MH2 is again intermediate. The source of variation on component 3 (9.8%) is unclear, but relative dimensions of the LP3 and LM3 appear contributory based on moderate loadings.

**[TABLE 7 and FIGURE 9 HERE]**

### **The Meta-Individual Comparison**

Finally, analysis was conducted at the individual level to address the potentially confounding issue of comparing within- (*A. sediba*) to among-group data (all other species). Expectation-maximization (EM) estimation (Dempster et al., 1977) was used to replace missing data in the four modern *H. sapiens* samples, where four or fewer of the 28 total MD and BL measurements (excluding the mostly unerupted M3s) were absent. The estimates were based on the five highest correlations for the absent value by sample. Little's (1988) test was used to determine whether these data were missing completely at random. If not, such cases were deleted; the result was a reduction in the effective number of modern individuals to 159 Bhils, 190 Garasias, 60 San, and 130 Pedi. From them, the abovementioned random samples were drawn that reflect the size and relative representation by dental element of the "average fossil hominin taxon." The latter, which is averaged across values for the six fossil comparative samples (e.g., see Table 2), consists of 94 individuals with nine UI1s, eight UI2s, 11 UCs, 14

UP3s, 14 UP4s, 16 UM1s, 11 UM2s, seven LI1s, seven LI2s, 11 LCs, 15 LP3s, 16 LP4s, 20 LM1s, and 21 LM2s. Therefore, a series of 94 replicate data sets were drawn randomly from each modern sample to obtain meta-individuals. To err on the side of caution, all were drawn separately by dental element from a sampling frame in which a random 15% set of individuals was removed prior to each sampling event. This same process was repeated for the comparative fossil samples. Most of these necessitated data sub-sampling like in the modern groups, while those of very small size, e.g., *H. habilis* (see Table 2), required repeated resampling from the same data set.

In the end, the 10 comparative samples comprise 94 meta-individuals apiece. Excluding the MD LI1 and LI2 dimensions (i.e., those absent in MH2), the average 26 measurements for each meta-individual were geometrically scaled with DM correction for TSA comparison to *A. sediba*. Because the latter species is represented by just one maxilla and mandible, to here yield a combined individual (i.e., MH1\_2), there is no variance in crown measurements; thus, it is not possible to create replicates as above. Instead, the pooled variance/covariance matrix of the other fossil hominins and modern humans was employed to place *A. sediba* in multi-component space relative to these taxa. Descriptive statistics for these comparative samples and meta-individuals, including the slightly different DM-scaled values from those in Table 3, are available from the authors and are planned for presentation elsewhere.

Component values are listed as before (Table 8), but the many meta-individuals dictate that only average group component scores (centroids) are plotted for each comparative sample and MH1\_2 (Fig. 10). Patterning clearly parallels the among-group results, particularly that of the maxilla (compare to Figs. 5 and 9). On component 1 (69.9% of the variance) relatively large posterior teeth, other than UM1 DM\_MD and LM1 DM\_BL values, are again responsible for the

location of the two *Paranthropus* centroids at the far end of the X axis (loadings 0.508 to 0.967). All others, the *H. sapiens* meta-individuals in particular, have the opposite pattern of relatively large anterior teeth (-0.651 to -0.944). On component 2 (14.9%), the large size of M1 to M2 that typifies *H. sapiens* separates species along the Y axis, as above. And on component 3 (5.3%), the lowest scorers on the Z axis, *H. ergaster*, MH1\_2, and to a lesser degree, *H. habilis*, share a long UM1 DM\_MD dimension based on one moderate loading (-0.480); high scorers do not have this attribute, but share relatively broad LM1s (0.418). Like the preceding analyses, *A. sediba* plots in an intermediate location relative to all others, here roughly equidistant between *H. sapiens* and the other *Homo* species.

**[TABLE 8 and FIGURE 10 HERE]**

## DISCUSSION

Together, the individual measurements and PCA components thoroughly characterize *A. sediba* and the comparative samples. That is, the apportionment, or patterning, of relative tooth size within and among samples of individuals is identified (Harris, 1997, 1998) based on the highly heritable actual and scaled MD and BL dimensions (Alvesalo and Tigerstedt, 1974; Townsend and Brown, 1980; Kieser, 1990; Dempsey et al., 1995; Dempsey and Townsend, 2001; Hlusko et al., 2002; Townsend et al., 2003; Baydas et al., 2005; Rizk et al., 2008). Plotting this patterning, in turn, visualizes among-sample phenetic variation to enable additional insight into the affinities of *A. sediba* to other species.

*Australopithecus sediba* appears roughly average (MH1) to below average (MH2) in absolute crown size compared to small- and large-toothed hominins (Tables 1-2); qualitatively, it most closely follows the tooth-by-tooth estimated crown area trend line (Figs. 2 and 6) of *A. afarensis*, as well as *H. habilis* – especially within the maxilla. The most obvious difference is

smaller canine and posterior tooth size toward the condition in later *Homo*. After size-correcting these measurements, *A. sediba* again appears somewhat similar to *A. afarensis* and *H. habilis* (Fig. 3b), as well as *A. africanus*.

Continuing to focus on the more complete MH1 maxillary dentition, the inter-sample phenetic affinities seen in the dendrogram of 16 corrected but correlated measurements (Fig. 3b) largely parallel those in Figure 4 from the uncorrelated principal components. Such continuity speaks to data constancy, regardless of analytical or illustrative method. As well, this maxillary output, excluding Pan (Table 5 and Fig. 5), is highly concordant with that from comparisons of meta-individuals with complete dentitions (i.e., 24 measurements) (Table 8 and Fig. 10); thus, at least in this study, direct comparison of within- (*A. sediba*) to among-group data (other species) provides plausible results. Together, these phenetic affinities appear generally concordant with those in dendrograms and cladograms from dental morphological (Irish et al., 2013, 2014) and craniodental traits (Berger et al., 2010). In these prior cases, *A. sediba* exhibits some similarity to *A. africanus*; previously the two were interpreted to be sister species within a South African australopith clade.

The TSA results suggest a closer relationship to the genus *Homo*. Of course, this phenetic affinity cannot be directly compared with relationships discerned in recent phylogenetic research, because of differences in sample composition and approach, but it does seem supportive. That is, using Bayesian analysis Dembo et al. (2015) posited that the best supported hypothesis is “one in which *A. sediba* is the sister taxon of a clade comprising all *Homo* species;” not surprisingly, given the use of the same character dataset, this finding was said to be “consistent with Berger et al.’s (2010) conclusion that *A. sediba* groups with *Homo* and may be its ancestor” (Dembo et al., 2015 p 3).

With regard to other samples: 1) *Pan* serves to demonstrate how the geometrically-scaled crown measurements and TSA analyses yield likely inter-sample affinities (Figs. 3b-4 and 8), contra comparisons based on absolute crown size (Fig. 3a), 2) both *P. robustus* and *P. boisei* are divergent as would be expected because of their highly specialized dentitions (Figs. 3b-5, 8-10) and, again focusing on the maxillary- and combined-dentition results 3) *A. afarensis* appears to be phenetically most akin to *A. africanus* then, to a much lesser degree, *H. habilis* and *A. sediba* and/or *H. erectus* (Figs. 3b-5 and 10). These odontometric phenetic affinities do not agree with previous results (Berger et al., 2010; Irish et al., 2013, 2014) where, for example, *A. afarensis* was linked with the *Paranthropus* species based on several shared, mass-additive molar traits.

In sum, size-corrected results from crown diameters, which derive from different genetic pathways (Dassule et al., 2000; Shimizu et al., 2004; Sperber, 2006; Townsend et al., 2009) than previously-analyzed characters, emulate many findings reported for the crania, dentition, and post-crania (i.e., Berger et al., 2010; Carlson et al., 2011; Kivell et al., 2011; Kibii et al., 2011; Zipfel et al., 2011; Churchill et al., 2013; de Ruiter et al., 2013; Irish et al., 2013, 2014; Schmid et al., 2013; Williams et al., 2013). *Australopithecus sediba* has some commonalities with other australopiths, but perhaps paralleling recent phylogenetic findings (Dembo et al., 2015) it shares several features with later *Homo*, including such synapomorphies as the aforementioned dental morphological and metric features and, among others, small mandibular corpus width, a highly flexible spine, a narrow waist, and a notch on the lateral plateau of the proximal tibiae (Berger et al., 2010; de Ruiter et al., 2013; Irish et al., 2013, 2014; Schmid et al., 2013; Williams et al., 2013); such links may be reflected in the above figures by the proximity of MH1 and MH2 to the samples of *H. habilis*, *H. erectus*, and *H. sapiens*. In fact, Dembo et al. (2015) suggest that *A. sediba* could be assigned to the genus *Homo*.

Nevertheless, determining the relationships of *A. sediba*, whether phenetic or cladistic, remains a work in progress. The most obvious concern is sample size; two partial dentitions obviously cannot capture the range of intraspecific variation necessary for comprehensive interspecific comparisons. Thus, the usual paleoanthropological caveat applies: recovery of more *A. sediba* (and other Plio-Pleistocene hominin) fossils is essential to promote more definitive conclusions.

### **ACKNOWLEDGMENTS**

We thank Kristian Carlson of the University of the Witwatersrand, Paul Tafforeau from the European Synchrotron Radiation Facility (ESRF), in Grenoble, and Isabelle De Groote of Liverpool John Moores University for their input. All of the individuals at various institutions from which the recent African data were collected cannot be listed here – but their help is greatly appreciated. With respect to the entire project, we thank the South African Heritage Resource agency for permits to work at Malapa; the Nash family for granting access to the site and continued support of research on their reserve; the South African Department of Science and Technology, African Origins Platform (AOP), Gauteng Provincial Government, the South African National Research Foundation, Institute for Human Evolution, University of the Witwatersrand, University of the Witwatersrand's Vice Chancellor's Discretionary Fund, National Geographic Society, Palaeontological Scientific Trust, Andrew W. Mellon Foundation, Ford Foundation, U.S. Diplomatic Mission to South Africa, French Embassy of South Africa, A.H. Schultz Foundation, Duke University, Ray A. Rothrock '77 Fellowship and IRTAG of Texas A&M University, and the Oppenheimer and Ackerman families and Sir Richard Branson for funding; the University of the Witwatersrand's Schools of Geosciences and Anatomical Sciences and Bernard Price Institute for Palaeontology for support and facilities; Gauteng

Department of Agriculture, Conservation and Environment and the Cradle of Humankind Management Authority; our respective universities for ongoing support. For access to other comparative specimens, E. Mbua, P. Kiura, V. Iminjili, and the National Museums of Kenya, B. Billings, B. Zipfel, and the School of Anatomical Sciences at University of the Witwatersrand, and S. Potze, L.C. Kgasi, and the Ditsong Museum. For technical and material support, Duke University, the University of Zurich 2009 and 2010 Field Schools, A.B. Taylor, C.E. Terhune and C.E. Wall. Numerous individuals were involved in the preparation and excavation of these fossils, including C. Dube, C. Kemp, M. Kgasi, M. Languza, J. Malaza, G. Mokoma, P. Mukanela, T. Nemvhundi, M. Ngcamphalala, S. Jirah, S. Tshabalala, and C. Yates. Others who have given significant support include B. de Klerk, W. Lawrence, C. Steininger, B. Kuhn, L. Pollarolo, B. Zipfel, J. Kretzen, D. Conforti, J. McCaffery, C. Dlamini, H. Visser, R. McCrae-Samuel, B. Nkosi, B. Louw, L. Backwell, F. Thackeray, and M. Peltier. J. Smilg facilitated computed tomography scanning of the specimens. Last, but certainly not least, we thank the ESRF for granting beam time on the ID17 and ID19 for experiment # EC521.



## LITERATURE CITED

- Aldenderfer MS, Blashfield RK. 1984. Cluster analysis. Beverly Hills: Sage Publications.
- Alvesalo L, Tigerstedt PMA. 1974. Heritabilities of human tooth dimensions. *Hereditas* 77:311-318.
- Baab KL. 2008. The taxonomic implications of cranial shape variation in *Homo erectus*. *J Hum Evol* 54:827–847.
- Baab KL, McNulty KP, Rohlf FJ. 2012. The shape of human evolution: A geometric morphometrics perspective. *Evol Anthropol* 21:151-165.
- Baydas B, Oktay H, Dağsuyu IM. 2005. The effect of heritability on Bolton tooth-size discrepancy. *Eur J Orthodont* 27:98-102.
- Berger LR, de Ruiter DJ, Churchill SE, Schmid P, Carlson KJ, Dirks PH, Kibii JM. 2010. *Australopithecus sediba*: A new species of *Homo*-like australopith from South Africa. *Science* 328:195-204.
- Berger LR, Hawks J, de Ruiter D J, Churchill SE, Schmid P, Deleuzene LK, ... Skinner MM. 2015. *Homo naledi*, a new species of the genus *Homo* from the Dinaledi Chamber, South Africa. *Elife* 4:e09560.
- Braga J. 2016. Non-invasive imaging techniques In: Irish JD, Scott GR, editors. A companion to dental anthropology. New York: Wiley-Blackwell p 514-527.

- Brook AH, Griffin RC, Townsend G, Levisianos Y, Russell J, Smith RN. 2008. Variability and patterning in permanent tooth size of four human ethnic groups. *Arch Oral Biol* 54, Suppl 1:S79-S85.
- Brown F, Harris J, Leakey R, Walker A. 1985. Early *Homo erectus* skeleton from West Lake Turkana, Kenya. *Nature* 316:788-792.
- Carlson KJ, Stout D, Jashashvili T, de Ruiter DJ, Tafforeau P, Carlson K, Berger LR. 2011. The endocast of MH1, *Australopithecus sediba*. *Science* 333:1402-1407.
- Churchill SE, Holliday TW, Carlson KJ, Jashashvili T, Macias ME, Mathews S, Berger LR. 2013. The upper limb of *Australopithecus sediba*. *Science* 340:1233-1237.
- Copes LE, Schwartz GT. 2010. The scale of it all: postcanine tooth size, the taxon-level effect, and the universality of Gould's scaling law. *Paleobiology* 36(2):188-203.
- Corruccini RS. 1973. Size and shape in similarity coefficients based on metric characters. *Am J Phys Anthropol* 38:743-754.
- Darroch JN, Mosimann JE. 1985. Canonical and principal components of shape. *Biometrika* 72:241-252.
- Dassule HR, Lewis P, Bei M, Maas R, McMahon AP. 2000. Sonic Hedgehog regulates growth and morphogenesis of the tooth. *Development* 127:4775-4785.
- de Ruiter DJ. 2004. Undescribed hominin fossils from the faunal stores of the Transvaal Museum, South Africa. *Annals Transvaal Mus* 41:29-40.

de Ruiter DJ, DeWitt TJ, Carlson KB, Brophy JK, Schroeder L, Ackermann RR, Berger LR. 2013. Mandibular remains support taxonomic validity of *Australopithecus sediba*. Science 340:1232997.

Dembo M, Matzke NJ, Mooers, AØ, Collard M. 2015. Bayesian analysis of a morphological supermatrix sheds light on controversial fossil hominin relationships. Proc R Soc B 282:20150943.

Dempsey PJ, Townsend GC, Martin NG, Neale MC. 1995. Genetic covariance structure of incisor crown size in twins. J Dent Res 74:1389-1398.

Dempsey PJ, Townsend GC. 2001. Genetic and environmental contributions to variation in human tooth size. Heredity 86:685-693.

Dempster AP, Laird NM, Rubin DB. 1977. Maximum likelihood from incomplete data via the EM Algorithm. J R Stat Soc B 39:1-38.

Everitt B. 1980. Cluster analysis. New York: John Wiley and Sons.

Felsenstein J. 1985. Phylogenies and the comparative method. Am Nat 125:1-15.

Gabunia L, Vekua A. 1995. Plio-Pleistocene hominid from Dmanisi, east Georgia, Caucasus. Nature 373:509.

Garn SM, Brace CL, Cole PE. 1977. Use of crown areas in odontometric analyses. J Dent Res 56:876.

Gingerich PD, Schoeninger MJ. 1979. Patterns of tooth size variability in the dentition of primates. Am J Phys Anthropol 51:457-466.

- Gingerich PD, Smith BH. 1985. Allometric scaling in the dentition of primates and insectivores. In: Size and Scaling in Primate Biology, W.L. Jungers, editor. New York: Plenum Press. pp. 257-272.
- Gould SJ. 1975. On the scaling of tooth size in mammals. *Am Zool* 15(2):353-362.
- Grine FE. 1989. New hominid fossils from the Swartkrans formation (1979-1986 excavations): cranio-dental specimens. *Am J Phys Anthropol* 79:409-449.
- Grine FE, Daegling DJ. 1993. New mandible of *Paranthropus robustus* from Member 1, Swartkrans Formation, South Africa. *J Hum Evol* 24:319-333.
- Grine, FE, Strait, DS. 1994. New hominid fossils from Member 1 "Hanging Remnant", Swartkrans Formation, South Africa. *J Hum Evol* 26:57-75.
- Haeussler AM, Irish JD, Morris D, Turner CG I. 1989. Morphological and metrical comparison of San and Central Sotho dentitions from southern Africa. *Am J Phys Anthropol* 78:115-122.
- Harris EF. 1997. A strategy for comparing odontometrics among groups. *Dental Anthropol* 12:1-6.
- Harris EF. 1998. Ontogenetic and intraspecific patterns of odontometric associations in humans. In: Lukacs JR. Eds. Human Dental Development, Morphology, and Pathology: A Tribute to Albert A. Dahlberg. Eugene: University of Oregon Anthropological Papers, Number 54. p 299-346.

Harris EF, Bailit HL. 1988. A principal components analysis of human odontometrics. *Am J Phys Anthropol* 75:87-99.

Harris EF, Harris JT. 2007. Racial differences in tooth crown size gradients within morphogenetic fields. *Rev Estomat* 15(suppl): 7-16.

Harris EF, Rathbun TA. 1991. Ethnic differences in apportionment of tooth sizes. In: V, editors. *Advances in dental anthropology*. New York: Alan R Liss. p 121-142.

Harvey PH, Pagel M, Rees J. 1991. Mammalian metabolism and life histories. *Am Nat* 137:556-566.

Hemphill BE. 2016a. Measurement of tooth size (odontometrics) In: Irish JD, Scott GR. Eds. *A Companion to Dental Anthropology*. New York: Wiley-Blackwell p 287-310.

Hemphill BE. 2016b. Assessing odontometric variation among populations In: Irish JD, Scott GR. Eds. *A Companion to Dental Anthropology*. New York: Wiley-Blackwell p 311-336.

Hemphill BE, Lukacs JR, Rami Reddy V. 1992. Tooth size apportionment among contemporary Indians: Factors of caste, language, and geography. *J Hum Ecol* 2:231-253.

Hlusko LJ, Weiss KM, Mahaney MC. 2002. Statistical genetic comparison of two techniques for assessing molar crown size in pedigreed baboons. *Am J Phys Anthropol* 117:182-189.

Irish JD. 1993. Biological affinities of late Pleistocene through modern African aboriginal populations: The dental evidence. Ph.D. Dissertation, Arizona State University, Tempe

Irish JD, Guatelli-Steinberg D, Legge SS, de Ruiter DJ, Berger LR. 2013. Dental morphology and the phylogenetic 'place' of *Australopithecus sediba*. *Science* 340:1233062.

Irish JD, Guatelli-Steinberg D, Legge SS, de Ruiter DJ, Berger LR. 2014. News and views: Response to 'Non-metric dental traits and hominin phylogeny' by Carter et al, with additional information on the Arizona State University Dental Anthropology System and phylogenetic 'place' of *Australopithecus sediba*. J Hum Evol 69:129-134.

Irish JD, Hemphill BE. 2001. Les Canaries ont-elles été colonisées par les Berbères d'Afrique du Nord? La contribution de l'analyse odontométrique In: Hadjouis D, Mafart B, editors. La Paléo-odontologie: Analyses et méthodes d'étude Collection paléoanthropologie et paléopathologie osseuse. Paris: Editions Artcom p 122-137.

Irish JD, Kenyhercz M. 2013. Size does matter: Variation in tooth size apportionment among major regional North and sub-Saharan African populations. Dental Anthropol 26:38-44.

Johanson DC, White TD, Coppens Y. 1982. Dental remains from the Hadar Formation, Ethiopia: 1974-1977 collections. Am J Phys Anthropol 57:545-603.

Jungers WL, Falsetti AB, Wall CE. 1995. Shape, relative size, and size-adjustments in morphometrics. Yearb Phys Anthropol 38:137-161.

Kato A, Ohno N. 2009. Construction of three-dimensional tooth model by micro-computed tomography and application for data sharing. Clin Oral Investigations 13:43-46.

Kay RF, Plavcan JM, Glander KE, Wright PC. 1988. Sexual selection and canine dimorphism in new world monkeys. Am J Phys Anthropol 77(3):385-397.

Kibii JM, Churchill SE, Schmid P, Carlson KJ, Reed ND, de Ruiter DJ, Berger LR. 2011. A partial pelvis of *Australopithecus sediba*. Science 333:1407-1411.

Kieser, JA 1990. Human adult odontometrics. Cambridge: Cambridge University Press.

Kimbel WH, Johanson DC, Rak Y. 1997. Systematic assessment of a maxilla of *Homo* from Hadar, Ethiopia Am J Phys Anthropol 103:235-262.

Kimbel WH, Rak Y, Johanson DC. 2004. The skull of *Australopithecus afarensis*. Oxford: Oxford University Press.

Kivell TL, Kibii JM, Churchill SE, Schmid P, Berger LR. 2011. *Australopithecus sediba* hand demonstrates mosaic evolution of locomotor and manipulative abilities. Science 333:1411.

Leigh SR. 1992. Patterns of variation in the ontogeny of primate body size dimorphism. J Hum Evol 23(1):27-50.

Little RJA. 1988. A test of missing completely at random for multivariate data with missing values. J AM Stat Assoc 83:1198-1202.

Lordkipanidze D, de León MSP, Margvelashvili A, Rak Y, Rightmire GP, Vekua A, Zollikofer CP. 2013. A complete skull from Dmanisi, Georgia, and the evolutionary biology of early *Homo*. Science, 342:326-331.

Lordkipanidze D, Vekua A, Ferring R, Rightmire GP, Zollikofer CP, Ponce de León MS, Agusti J, Kiladze G, Mouskhelishvili A, Nioradze M, Tappen M. 2006. A fourth hominin skull from Dmanisi, Georgia. Anat Rec A Discov Mol Cell Evol Biol. 288A:1146–1157.  
doi:10.1002/ara.20379.

- Lukacs JR, Hemphill BE. 1993. Odontometry and biological affinity in South Asia: Analysis of three ethnic groups from Northwest India. *Hum Biol* 65:279-325.
- Mahler PE. 1973. Metric variation in the pongid dentition. PhD thesis, University of Michigan.
- Martinón-Torres M, de Castro JMB, Gómez-Robles A, Margvelashvili A, Prado L, Lordkipanidze D, Vekua A. 2008. Dental remains from Dmanisi (Republic of Georgia): morphological analysis and comparative study. *J Hum Evol* 55:249-273.
- Mitteroecker P, Gunz P. 2009. Advances in geometric morphometrics. *Evol Biol* 36:235-247.
- Moggi-Cecchi J, Grine FE, Tobias PV. 2006. Early hominid dental remains from Members 4 and 5 of the Sterkfontein Formation (1966-1996 excavations): Catalogue, individual associations, morphological descriptions, and initial metrical analysis. *J Hum Evol* 50:239-328.
- Moorrees CFA, Reed RB. 1964. Correlations among crown diameters of human teeth. *Archives Oral Biol* 9:685-697.
- Olejniczaki AJ, Grine F. 2006. Assessment of the accuracy of dental enamel thickness measurements using microfocal X-ray computed tomography. *Anat Rec A* 288:263–75.
- Pagel M, Harvey P. 1988. The taxon-level problem in the evolution of mammalian brain size: facts and artifacts. *Am Nat* 132:344-359.
- Pagel M, Harvey. P. 1989. Taxonomic differences in the scaling of brain on body weight among mammals. *Science* 244:1589-1593.



Penrose LS. 1954. Distance, size and shape. *Ann Eugenics* 18:337-343.

Pilloud MA, Hefner JT, Hanihara T, Hayashi A. 2014. The use of tooth crown measurements in the assessment of ancestry. *J Forensic Sci* 59(6):1493-1501.

Plavcan JM. 2001. Sexual dimorphism in primate evolution. *Yrbk Phys Anthropol* 33:25-53.

Prat S, Brugal JP, Tiercelin JJ, Barrat JA, Bohn M, Delagnes A, Roche, H. 2005. First occurrence of early *Homo* in the Nachukui formation (West Turkana, Kenya) at 2.3-2.4 Myr. *J Hum Evol* 49:230-240.

Rahman NA. 1962. On the sampling distribution of the studentized Penrose measure of distance. *Ann Hum Genetics* 26:97-106.

Rightmire GP, Lordkipanidze D, Vekua A. 2006. Anatomical descriptions, comparative studies and evolutionary significance of the hominin skulls from Dmanisi, Republic of Georgia. *J Hum Evol* 50:115–141 doi:101016/j.jhevol200507009.

Rightmire GP, Lordkipanidze D. 2010. The first hominin colonization of Eurasia. In: Fleagle JG, Shea JJ, Grine FE, Baden AL, Leakey RE, editors. *Out of Africa I*. New York: Springer. p 225–243.

Rizk OT, Amugongo SK, Mahaney MC, Hlusko LJ. 2008. The quantitative genetic analysis of primate dental variation: History of the approach and prospects for the future. In: Irish JD, Nelson GC, editors. *Technique and application in dental anthropology*. Cambridge: Cambridge University Press p 317-346.

- Robinson JT. 1956. The dentition of the Australopithecinae. Transvaal Museum Memoir No 9. Pretoria: Transvaal Museum.
- Romesburg CH. 1984. Cluster analysis for researchers. Belmont, CA: Lifetime Learning Publications.
- Schmid P, Churchill SE, Nalla S, Weissen E, Carlson KJ, de Ruiter DJ, Berger LR. 2013. Mosaic morphology in the thorax of *Australopithecus sediba*. Science 340:1234598.
- Shimizu T, Oikawa H, Han J, Kurose E, Maeda T. 2004. Genetic analysis of crown size in the first molars using SMXA recombinant inbred mouse strains. J Dent Res 83:45-49.
- Smith RJ. 1981a. Interspecific scaling of maxillary canine size and shape in female primates: Relationships to social structure and diet. J Hum Evol 10(2):165-173.
- Smith RJ. 1981b. On the definition of variables in studies of primate dental allometry. Am J Phys Anthropol 55(3):323-329.
- Sperber GH. 2006. The genetics of odontogenesis: implications in dental anthropology and palaeo-odontology. Trans Royal Soc S Afr 61:121-125.
- Strait DS, Grine FE 2004. Inferring hominoid and early hominid phylogeny using craniodental characters: the role of fossil taxa. J Hum Evol 47:399–452 doi:10.1016/j.jhevol.2004.08.008
- Suwa G, Asfaw B, Haile-Selassie Y, White T, Katoh S, WoldeGabriel G, Hart WK, Nakaya H, Beyene Y. 2007. Early Pleistocene *Homo erectus* fossils from Konso, southern Ethiopia. Anthropol Sci 115:133-151.

Suwa G, Kono RT, Simpson SW, Asfaw B, Lovejoy CO, White TD. 2009. Paleobiological implications of the *Ardipithecus ramidus* dentition. *Science* 326:94-99.

Tobias PV. 1967. Olduvai Gorge Vol 2, The cranium and maxillary dentition of *Australopithecus* (Zinjanthropus) *boisei*. Cambridge: Cambridge University Press.

Tobias PV. 1991. Olduvai Gorge Vol IV, The skulls, endocasts and teeth of *Homo habilis*. Cambridge: Cambridge University Press.

Toma T, Hanihara T, Sunakawa H, Haneji K, Ishida H. 2007. Metric dental diversity of Ryukyu Islanders: a comparative study among Ryukyu and other Asian populations. *Anthropol Sci* 115:119-131.

Townsend GC, Brown T. 1980. Dental symmetry in Australian Aborigines. *Hum Biol* 52:661–673.

Townsend G, Harris EF, Lesot H, Clauss F, Brook A. 2009. Morphogenetic fields within the human dentition: a new, clinically relevant synthesis of an old concept. *Arch Oral Biol* 54:S34-S44.

Townsend G, Richards L, Hughes T. 2003. Molar intercuspal dimensions: genetic input to phenotypic variation. *J Dent Res* 82:350-355.

White TD, WoldeGabriel G, Asfaw B, Ambrose S, Beyene Y, Bernor RL, ... Suwa G. 2006. Asa Issie, Aramis and the origin of *Australopithecus*. *Nature* 440:883-889.

Williams SA, Ostrofsky KR, Frater N, Churchill SE, Schmid P, Berger LR. 2013. The vertebral column of *Australopithecus sediba*. *Science* 340:1232996.

Wolpoff MH. 1971. Metric trends in hominid dental evolution, Case Western Reserve University Studies in Anthropology, No 2.

Wolpoff MH. 1985. Tooth size-body size scaling in a human population: Theory and practice of an allometric analysis. In: Size and Scaling in Primate Biology, W.L. Jungers, editor. New York: Plenum Press. pp. 273-318.

Wood BA. 1991. Koobi Fora Research Project: Volume 4, hominid crania remains. Oxford: Clarendon Press.

Zipfel B, DeSilva JM, Kidd RS, Carlson KJ, Churchill SE, Berger LR. 2011. The foot and ankle of *Australopithecus sediba*. Science 333:1417-1420.

#### FOOTNOTE

<sup>1</sup>In this (Fig. 4) and subsequent three-dimensional plots the X axis is oriented vertically so the *H. sapiens* sample is positioned on the right to standardize comparison.

**Table 1.** Mesiodistal (MD) and buccolingual (BL) maxillary (upper) and mandibular (lower) maximum crown diameters in millimeters for the two *Australopithecus sediba* specimens (values in **bold** are either revised or previously unpublished measurements).

	Specimen MH1				Specimen MH2			
	Right		Left		Right		Left	
	MD	BL	MD	BL	MD	BL	MD	BL
UI1	10.1	6.9						
UI2			<b>7.2<sup>2</sup></b>	<b>6.6<sup>1</sup></b>				
UC	9.0	8.8						
UP3	<b>8.9</b>	<b>11.1</b>	9.0	11.2 <sup>1</sup>				
UP4	<b>9.2<sup>1</sup></b>	<b>12.1<sup>1</sup></b>	<b>9.3</b>	12.1 <sup>1</sup>				
UM1	<b>12.7</b>	<b>12.4<sup>2</sup></b>	12.9	12.0 <sup>1</sup>				
UM2	<b>13.0</b>	<b>13.5</b>	12.9	13.7 <sup>1</sup>				
UM3	<b>13.1<sup>1</sup></b>	<b>13.6<sup>1</sup></b>	13.3 <sup>1</sup>	14.1 <sup>1</sup>	<b>12.6<sup>2</sup></b>	12.9 <sup>2</sup>		
LI1						<b>5.9</b>		
LI2						<b>6.6</b>		
LC			8.0	<b>8.6</b>	<b>7.3</b>	<b>7.4</b>		
LP3	<b>8.0<sup>1</sup></b>				<b>8.1<sup>2</sup></b>	<b>9.2</b>		
LP4	<b>8.4<sup>1</sup></b>				<b>8.8<sup>2</sup></b>	<b>9.7</b>		
LM1	<b>13.1<sup>2</sup></b>	<b>11.5</b>			<b>13.1<sup>2</sup></b>	<b>11.3</b>		
LM2	<b>14.5</b>	<b>13.2</b>			<b>14.4<sup>2</sup></b>	<b>12.3</b>		
LM3	14.9	<b>13.6<sup>3</sup></b>			<b>14.9<sup>2</sup></b>	12.7	<b>14.8<sup>2</sup></b>	12.5

<sup>1</sup>Measurement based on synchrotron scan because actual crown is unerupted or obscured by matrix (see text for details).  
<sup>2</sup>Estimated maximum diameter of fractured or worn crown.  
<sup>3</sup>From 3D print generated from scan of unerupted tooth

**Table 2.** Mean mesiodistal (MD) and buccolingual (BL) maxillary (upper) and mandibular (lower) maximum crown diameters in mm for the comparative hominin and *Pan* samples<sup>1</sup>.

	<i>A. africanus</i>		<i>A. afarensis</i>		<i>P. robustus</i>		<i>P. boisei</i>		<i>H. habilis</i>		<i>H. erectus</i>		<i>H. sapiens</i>		<i>Pan troglodytes</i>	
	MD	BL	MD	BL	MD	BL	MD	BL	MD	BL	MD	BL	MD	BL	MD	BL
<b>UI1</b>	10.5 (8) <sup>2</sup>	8.4 (8)	10.7 (7)	8.4 (8)	8.8 (17)	7.2 (17)	9.2 (5)	7.0 (5)	10.8 (4)	7.5 (4)	11.4 (3)	7.8 (3)	8.6 (358)	7.0 (412)	11.7 (64)	9.4 (64)
<b>UI2</b>	6.8 (10)	6.9 (10)	7.5 (9)	7.2 (9)	6.7 (12)	6.8 (12)	7.9 (5)	6.6 (5)	7.2 (6)	6.8 (6)	8.1 (5)	7.6 (5)	6.8 (388)	6.3 (430)	8.6 (44)	8.6 (44)
<b>UC</b>	10.0 (13)	10.3 (13)	9.9 (15)	10.8 (15)	8.4 (26)	9.2 (26)	8.6 (5)	8.8 (5)	9.5 (6)	9.9 (6)	9.8 (6)	9.8 (6)	7.5 (554)	8.1 (575)	11.1 (60)	12.5 (60)
<b>UP3</b>	9.2 (22)	12.8 (22)	8.8 (12)	12.4 (10)	9.7 (28)	13.9 (28)	10.5 (9)	14.4 (9)	9.1 (9)	12.0 (9)	8.8 (10)	12.5 (10)	7.0 (653)	9.3 (668)	8.0 (70)	10.3 (70)
<b>UP4</b>	9.3 (14)	13.5 (14)	9.1 (18)	12.4 (12)	10.4 (31)	15.0 (31)	11.6 (4)	16.3 (4)	9.2 (9)	12.0 (9)	8.5 (7)	11.9 (7)	6.7 (631)	9.2 (658)	7.2 (49)	10.1 (49)
<b>UM1</b>	12.9 (19)	13.9 (19)	12.0 (16)	13.4 (13)	13.1 (34)	14.1 (34)	14.1 (13)	15.0 (13)	12.9 (13)	13.0 (13)	12.8 (12)	13.3 (11)	10.4 (609)	11.2 (718)	10.4 (70)	11.4 (70)
<b>UM2</b>	14.0 (20)	15.7 (20)	12.9 (10)	14.6 (11)	14.1 (26)	15.7 (26)	15.5 (8)	16.8 (8)	13.1 (10)	14.6 (10)	12.7 (8)	13.4 (8)	9.9 (659)	11.3 (714)	10.3 (50)	11.6 (50)
<b>UM3</b>	14.0 (24)	15.9 (24)	12.7 (11)	14.5 (11)	14.7 (30)	16.4 (30)	14.1 (5)	17.4 (5)	12.6 (8)	14.6 (8)	12.4 (5)	14.0 (5)	8.9 (427)	11.0 (458)	9.6 (57)	11.0 (57)

Table 2. Continued

	<i>A. africanus</i>		<i>A. afarensis</i>		<i>P. robustus</i>		<i>P. boisei</i>		<i>H. habilis</i>		<i>H. erectus</i>		<i>H. sapiens</i>		<i>Pan troglodytes</i>	
	MD	BL	MD	BL	MD	BL	MD	BL	MD	BL	MD	BL	MD	BL	MD	BL
LI1	6.1 (9)	6.5 (9)	6.7 (7)	7.1 (8)	5.4 (10)	6.1 (10)	5.3 (9)	6.7 (9)	6.5 (2)	6.9 (2)	5.7 (4)	6.5 (4)	5.2 (335)	5.7 (349)	7.8 (62)	8.7 (62)
LI2	7.2 (10)	7.8 (10)	6.7 (7)	8.0 (6)	6.5 (7)	6.6 (7)	5.8 (4)	7.2 (4)	7.7 (2)	7.5 (2)	7.2 (8)	7.2 (8)	5.8 (383)	6.1 (403)	8.4 (42)	9.1 (42)
LC	9.3 (23)	10.1 (23)	8.8 (13)	10.4 (16)	7.7 (20)	8.2 (20)	7.9 (11)	9.0 (11)	9.0 (3)	9.2 (3)	9.2 (6)	8.9 (6)	6.8 (449)	7.3 (475)	10.6 (61)	12.3 (61)
LP3	9.6 (18)	11.4 (18)	9.6 (27)	10.6 (26)	9.9 (24)	12.1 (24)	10.4 (10)	13.5 (10)	10.0 (3)	10.0 (3)	9.5 (11)	10.2 (12)	7.1 (499)	7.9 (517)	10.4 (69)	8.3 (69)
LP4	10.2 (24)	11.6 (24)	9.8 (24)	11.0 (21)	11.0 (22)	12.8 (22)	12.9 (19)	13.3 (18)	10.5 (3)	10.9 (3)	8.8 (9)	9.9 (9)	7.2 (469)	8.2 (510)	7.9 (48)	8.6 (48)
LM1	14.0 (27)	13.0 (27)	13.1 (32)	12.6 (26)	14.5 (33)	13.5 (33)	15.5 (19)	14.0 (19)	13.8 (5)	11.8 (5)	13.0 (16)	11.7 (16)	11.3 (443)	10.4 (533)	10.9 (70)	9.7 (70)
LM2	15.7 (35)	14.5 (35)	14.3 (31)	13.4 (27)	16.0 (26)	14.8 (26)	17.5 (20)	15.9 (20)	15.0 (5)	13.4 (5)	13.6 (16)	12.1 (16)	10.7 (462)	10.2 (547)	11.3 (50)	10.5 (50)
LM3	16.3 (31)	14.6 (31)	15.3 (26)	13.5 (23)	16.8 (31)	14.5 (31)	18.0 (26)	15.4 (26)	15.3 (5)	13.0 (5)	13.9 (10)	12.2 (11)	10.5 (319)	9.9 (343)	10.7 (58)	10.2 (58)

<sup>1</sup>Odontometric data from directly-recorded (by DJD and JDI) and published measurements (See references in text).

<sup>2</sup>Values in parentheses identify the number of teeth measured to calculate the mean diameter.



**Table 3.** DM\_RAW size-corrected<sup>1</sup> mesiodistal (MD) and buccolingual (BL) diameters for the comparative samples used in tooth size apportionment analyses.

	Specimen MH1		<i>A. africanus</i>		<i>A. afarensis</i>		<i>P. robustus</i>		<i>P. boisei</i>		<i>H. habilis</i>		<i>H. erectus</i>		<i>H. sapiens</i>		<i>Pan troglodytes</i>	
	MD	BL	MD	BL	MD	BL	MD	BL	MD	BL	MD	BL	MD	BL	MD	BL	MD	BL
<b>UI1</b>	0.99	0.67	0.94	0.75	0.99	0.78	0.80	0.65	0.80	0.61	1.02	0.71	1.07	0.73	1.00	0.82	1.17	0.94
<b>UI2</b>	0.70	0.64	0.61	0.62	0.69	0.67	0.61	0.62	0.68	0.57	0.68	0.64	0.76	0.71	0.80	0.74	0.86	0.86
<b>UC</b>	0.88	0.86	0.90	0.93	0.91	1.00	0.76	0.84	0.75	0.76	0.89	0.93	0.92	0.93	0.88	0.95	1.11	1.25
<b>UP3</b>	0.87	1.09	0.83	1.15	0.81	1.15	0.88	1.26	0.91	1.25	0.86	1.13	0.82	1.17	0.82	1.09	0.80	1.03
<b>UP4</b>	0.91	1.18	0.84	1.21	0.84	1.15	0.95	1.36	1.01	1.41	0.87	1.13	0.79	1.11	0.78	1.08	0.72	1.01
<b>UM1</b>	1.25	1.19	1.16	1.25	1.11	1.24	1.19	1.28	1.22	1.30	1.22	1.22	1.20	1.24	1.22	1.31	1.04	1.14
<b>UM2</b>	1.27	1.33	1.26	1.41	1.19	1.35	1.28	1.43	1.34	1.46	1.23	1.37	1.19	1.25	1.16	1.32	1.02	1.06
<b>UM3</b>	1.29	1.35	1.26	1.43	1.17	1.34	1.34	1.49	1.22	1.51	1.18	1.37	1.16	1.31	1.04	1.29	0.96	1.10

Table 3. Continued

	Specimen MH2		<i>A. africanus</i>		<i>A. afarensis</i>		<i>P. robustus</i>		<i>P. boisei</i>		<i>H. habilis</i>		<i>H. erectus</i>		<i>H. sapiens</i>		<i>Pan troglodytes</i>	
	MD	BL	MD	BL	MD	BL	MD	BL	MD	BL	MD	BL	MD	BL	MD	BL	MD	BL
LI1	*	0.61		0.57		0.65		0.54		0.56		0.64		0.64		0.68		0.89
LI2	*	0.68		0.69		0.73		0.59		0.60		0.69		0.70		0.73		0.92
LC	0.75	0.76	0.82	0.89	0.80	0.95	0.69	0.73	0.65	0.75	0.83	0.85	0.90	0.87	0.82	0.88	1.07	1.25
LP3	0.83	0.95	0.85	1.00	0.87	0.96	0.89	1.08	0.86	1.12	0.92	0.92	0.93	1.00	0.85	0.95	1.05	0.84
LP4	0.91	1.00	0.90	1.01	0.89	1.00	0.98	1.14	1.07	1.10	0.96	1.00	0.86	0.97	0.86	0.99	0.80	0.87
LM1	1.35	1.16	1.23	1.14	1.19	1.15	1.30	1.21	1.28	1.16	1.27	1.09	1.27	1.14	1.36	1.25	1.10	0.98
LM2	1.48	1.27	1.38	1.27	1.30	1.22	1.43	1.32	1.45	1.32	1.38	1.23	1.33	1.18	1.29	1.23	1.15	1.06
LM3	1.54	1.30	1.43	1.28	1.39	1.23	1.50	1.30	1.49	1.28	1.41	1.20	1.36	1.19	1.26	1.19	1.09	1.04

<sup>1</sup>See main text for details  
\*Cannot be determined because of missing data in MH2 (see text).

**Table 4.** Component loadings<sup>1</sup>, eigenvalues, and the variance explained for size-corrected maxillary measurements in MH1 and the eight comparative samples.

Variable	Component		
	1	2	3
DM_MDUI1	<b>-0.946</b>	0.042	-0.242
DM_MDUI2	<b>-0.831</b>	0.419	-0.029
DM_MDUC	<b>-0.966</b>	-0.209	-0.104
DM_MDUP3	<b>0.863</b>	0.072	-0.255
DM_MDUP4	<b>0.938</b>	-0.086	-0.129
DM_MDUM1	<b>0.695</b>	<b>0.546</b>	-0.417
DM_MDUM2	<b>0.980</b>	-0.018	-0.135
DM_MDUM3	<b>0.862</b>	-0.330	-0.232
DM_BLUI1	<b>-0.951</b>	-0.045	0.247
DM_BLUI2	<b>-0.957</b>	0.119	0.081
DM_BLUC	<b>-0.951</b>	-0.238	0.129
DM_BLUP3	<b>0.864</b>	-0.098	0.326
DM_BLUP4	<b>0.923</b>	-0.146	0.162
DM_BLUM1	<b>0.664</b>	<b>0.510</b>	<b>0.521</b>
DM_BLUM2	<b>0.933</b>	-0.076	0.181
DM_BLUM3	<b>0.986</b>	-0.077	0.100
Eigenvalue	12.931	1.016	0.929
Variance (%)	80.820	6.352	5.808
Total Variance	80.820	87.172	92.980

<sup>1</sup>Values in bold-face indicate strong loadings (i.e.,  $\geq |0.5|$ ) as detailed in text.

**Table 5.** Component loadings<sup>1</sup>, eigenvalues, and the variance explained for size-corrected maxillary measurements in MH1 and seven comparative samples (excluding *Pan*).

Variable	Component		
	1	2	3
DM_MDUI1	-0.928	0.013	-0.321
DM_MDUI2	-0.663	<b>0.694</b>	0.099
DM_MDUC	-0.899	-0.298	-0.272
DM_MDUP3	<b>0.896</b>	0.361	-0.219
DM_MDUP4	<b>0.953</b>	0.099	-0.138
DM_MDUM1	0.212	<b>0.803</b>	-0.449
DM_MDUM2	<b>0.956</b>	0.005	-0.202
DM_MDUM3	<b>0.725</b>	-0.418	-0.426
DM_BLUI1	-0.887	-0.194	0.337
DM_BLUI2	-0.903	0.276	0.169
DM_BLUC	-0.878	-0.415	0.130
DM_BLUP3	<b>0.795</b>	-0.102	0.365
DM_BLUP4	<b>0.977</b>	-0.006	0.171
DM_BLUM1	0.225	0.368	<b>0.891</b>
DM_BLUM2	<b>0.846</b>	-0.234	0.263
DM_BLUM3	<b>0.965</b>	-0.179	0.139
Eigenvalue	10.963	2.048	1.880
Variance (%)	68.518	12.797	11.753
Total Variance	68.518	81.315	93.068

<sup>1</sup>Values in bold-face indicate strong loadings (i.e.,  $\geq |0.5|$ ) as detailed in text.

**Table 6.** Component loadings<sup>1</sup>, eigenvalues, and the variance explained for size-corrected mandibular measurements in MH2 and the eight comparative samples.

Variable	Component		
	1	2	3
DM_MDLI1	*	*	*
DM_MDLI2	*	*	*
DM_MDLC	-0.972	0.079	-0.064
DM_MDLP3	-0.853	-0.394	0.090
DM_MDLP4	0.807	-0.485	0.076
DM_MDLM1	0.727	<b>0.571</b>	0.025
DM_MDLM2	0.922	-0.063	-0.343
DM_MDLM3	0.929	-0.099	-0.331
DM_BLLI1	-0.969	0.048	0.056
DM_BLLI2	-0.981	0.100	-0.047
DM_BLLC	-0.973	-0.093	0.055
DM_BLLP3	0.846	-0.307	0.332
DM_BLLP4	0.912	-0.263	0.238
DM_BLLM1	0.757	<b>0.537</b>	0.357
DM_BLLM2	0.984	-0.045	0.027
DM_BLLM3	0.954	0.059	-0.182
Eigenvalue	11.413	1.214	0.582
Variance (%)	81.520	8.673	4.160
Total Variance	81.520	90.192	94.352

<sup>1</sup>Values in bold-face indicate strong loadings (i.e.,  $\geq |0.5|$ ) as detailed in text.

\*Cannot be determined because of missing data in MH2 (see text).

**Table 7.** Component loadings<sup>1</sup>, eigenvalues, and the variance explained for size corrected mandibular measurements in MH2 and seven comparative samples (excluding *Pan*).

Variable	Component		
	1	2	3
DM_MDLI1	*	*	*
DM_MDLI2	*	*	*
DM_MDLC	-0.925	-0.148	-0.082
DM_MDLP3	-0.314	-0.660	0.455
DM_MDLP4	0.824	-0.282	0.237
DM_MDLM1	0.137	0.791	0.038
DM_MDLM2	0.842	-0.039	-0.421
DM_MDLM3	0.829	-0.223	-0.464
DM_BLLI1	-0.915	0.236	0.027
DM_BLLI2	-0.947	0.132	-0.247
DM_BLLC	-0.870	-0.179	-0.034
DM_BLLP3	0.782	-0.121	0.440
DM_BLLP4	0.894	-0.042	0.361
DM_BLLM1	0.101	0.873	0.389
DM_BLLM2	0.950	0.138	0.019
DM_BLLM3	0.839	0.114	-0.425
Eigenvalue	8.566	2.131	1.384
Variance (%)	61.186	15.224	9.883
Total Variance	16.186	76.410	86.292

<sup>1</sup>Values in bold-face indicate strong loadings (i.e.,  $\geq |0.5|$ ) as detailed in text.

\*Cannot be determined because of missing data in MH2 (see text).

**Table 8.** Component loadings<sup>1</sup>, eigenvalues, and the variance explained for size corrected maxillary and mandibular measurements in *A. sediba* (MH1 and MH2) and meta-individuals comprising six fossil and four modern comparative samples (excluding *Pan*).

Variable	Component		
	1	2	3
DM_MDUI1	<b>-0.944</b>	0.131	-0.222
DM_MDUI2	<b>-0.865</b>	-0.413	-0.186
DM_MDUC	<b>-0.908</b>	0.211	-0.150
DM_MDUP3	<b>0.937</b>	-0.094	-0.225
DM_MDUP4	<b>0.951</b>	0.229	-0.024
DM_MDUM1	0.264	<b>-0.747</b>	-0.480
DM_MDUM2	<b>0.894</b>	0.215	-0.089
DM_BLUI1	<b>-0.938</b>	-0.177	0.186
DM_BLUI2	<b>-0.814</b>	-0.325	-0.336
DM_BLUC	<b>-0.920</b>	0.232	0.135
DM_BLUP3	<b>0.906</b>	0.103	-0.276
DM_BLUP4	<b>0.967</b>	0.127	0.001
DM_BLM1	<b>0.508</b>	<b>-0.796</b>	-0.025
DM_BLM2	<b>0.954</b>	0.042	0.061
DM_MDLI1	*	*	*
DM_MDLI21	*	*	*
DM_MDLC	<b>-0.854</b>	0.359	-0.230
DM_MDLP3	<b>0.722</b>	0.493	-0.374
DM_MDLP4	<b>0.963</b>	0.124	0.124
DM_MDLM1	<b>0.578</b>	<b>-0.711</b>	0.006
DM_MDLM2	<b>0.877</b>	0.344	0.021
DM_BLLI1	<b>-0.651</b>	<b>-0.502</b>	0.182
DM_BLLI2	<b>-0.906</b>	0.113	0.229
DM_BLLC	<b>-0.758</b>	0.479	0.341
DM_BLLP3	<b>0.880</b>	0.177	0.043
DM_BLLP4	<b>0.962</b>	-0.027	0.202
DM_BLLM1	0.363	<b>-0.769</b>	0.418
DM_BLLM2	<b>0.907</b>	-0.005	0.327
Eigenvalue	18.182	3.879	1.377
Variance (%)	69.929	14.921	5.297
Total Variance	69.929	84.850	90.147

<sup>1</sup>Values in bold-face indicate strong loadings (i.e.,  $\geq |0.5|$ ) as detailed in text.

\*Not determined because of missing data in MH2 (see text).



Figure 1. Right maxillary dentition of MH1 *A. sediba*, on which previously unpublished crown dimensions were taken. Note partially impacted UP4 and damaged UM1. See main text for details. Photograph by JDI. 110x203mm (300 x 300 DPI)



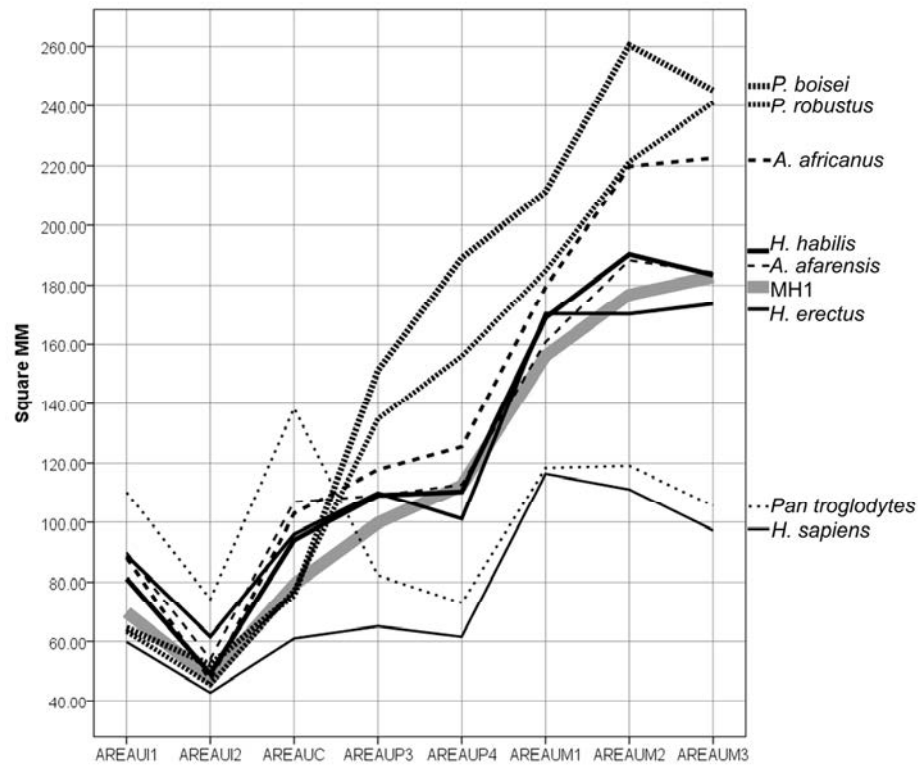


Figure 2. Line plot showing tooth-by-tooth trends in absolute occlusal surface areas (MD x BL) of the maxillary dentition in mm<sup>2</sup> by sample. See text for sample compositions.  
121x97mm (300 x 300 DPI)

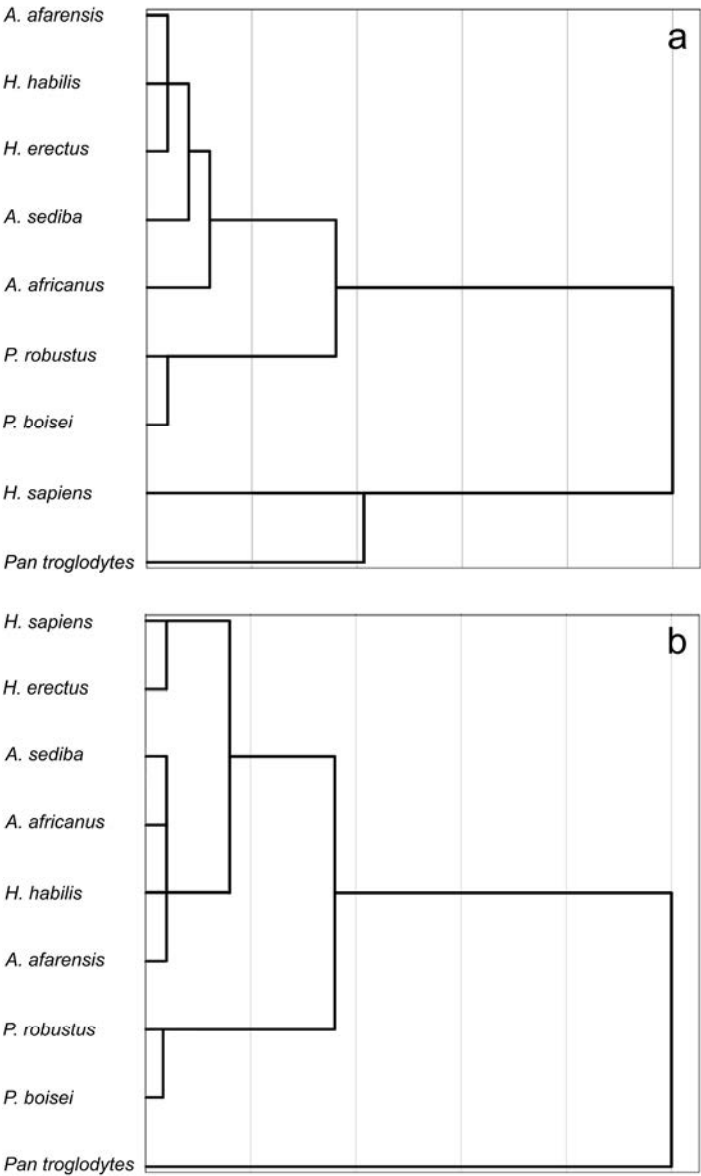


Figure 3. (a) Average linkage cluster analysis dendrogram based on uncorrected MD and BL dimensions of the maxillary teeth in *A. sediba* and the eight comparative samples. (b) Average linkage cluster dendrogram based on 16 DM\_RAW size-corrected MD and BL dimensions of the maxillary teeth in *A. sediba* and eight comparative samples. See text for methodological details and sample compositions.  
203x346mm (300 x 300 DPI)

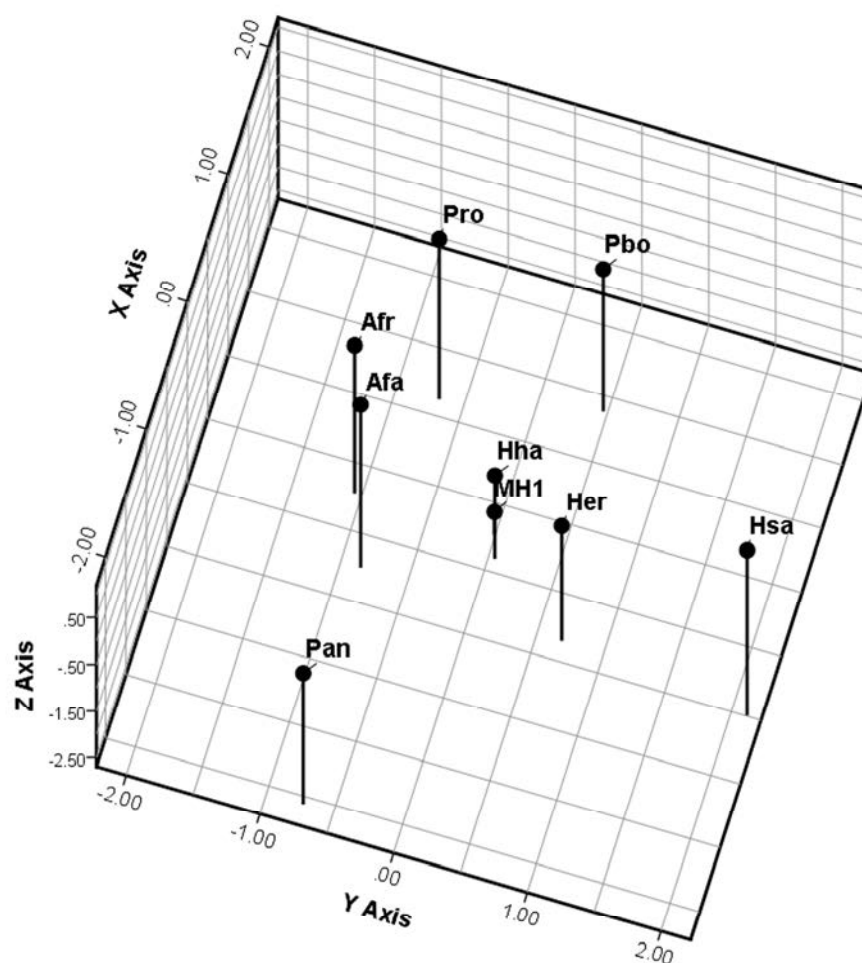


Figure 4. Three-dimensional ordination of retained principal component scores for tooth size apportionment in the maxillary dentition of *A. sediba* (MH1) and eight comparative samples. Accounts for 92.9% of the total variance (80.8% on X axis, 6.4% on Y axis, and 5.8% on Z axis). Afa = *A. afarensis*, Afr = *A. africanus*, Her = *H. erectus*, Hha = *H. habilis*, Hsa = *H. sapiens*, Pan = *Pan troglodytes*, Pbo = *P. boisei*, Pro = *P. robustus*. See text for methodological details, component descriptions, and sample compositions.

159x166mm (300 x 300 DPI)

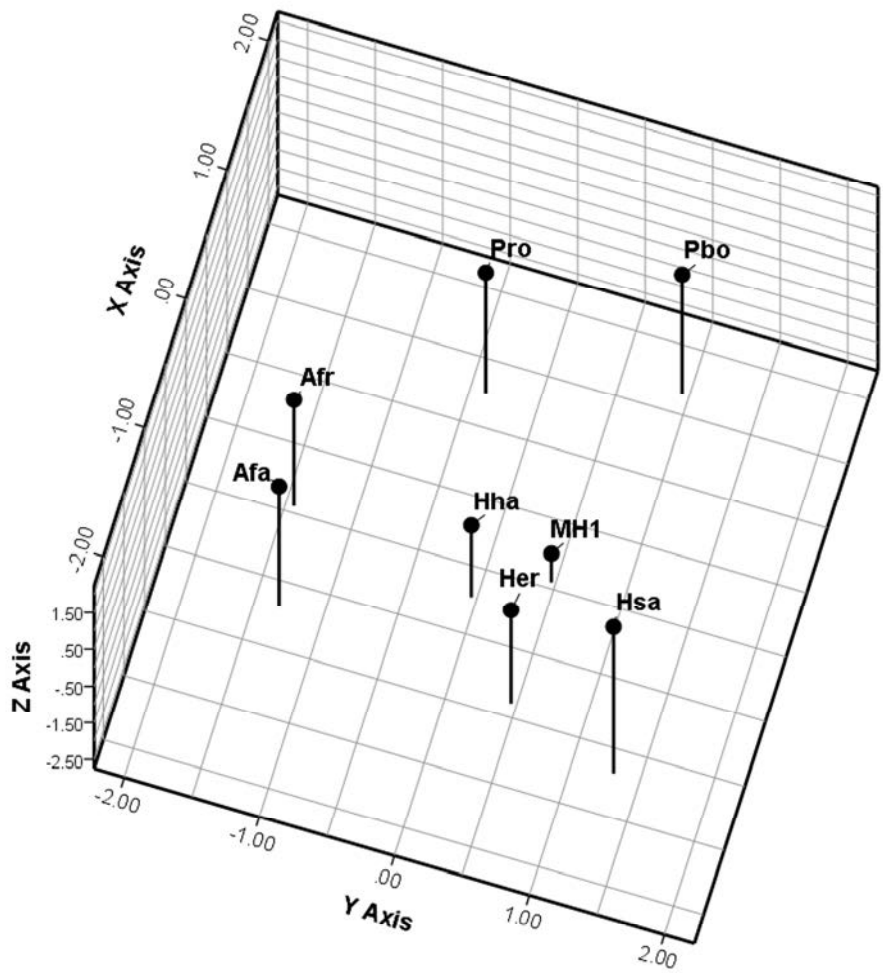


Figure 5. Three-dimensional ordination of retained principal component scores for tooth size apportionment in the maxillary dentition of *A. sediba* (MH1) and seven comparative hominin samples (i.e., excluding *Pan*). Accounts for 93.1% of the total variance (68.5% on X axis, 12.8% on Y axis, and 11.8% on Z axis. Afa = *A. afarensis*, Afr = *A. africanus*, Her = *H. erectus*, Hha = *H. habilis*, Hsa = *H. sapiens*, Pan = *Pan troglodytes*, Pbo = *P. boisei*, Pro = *P. robustus*.  
160x170mm (300 x 300 DPI)

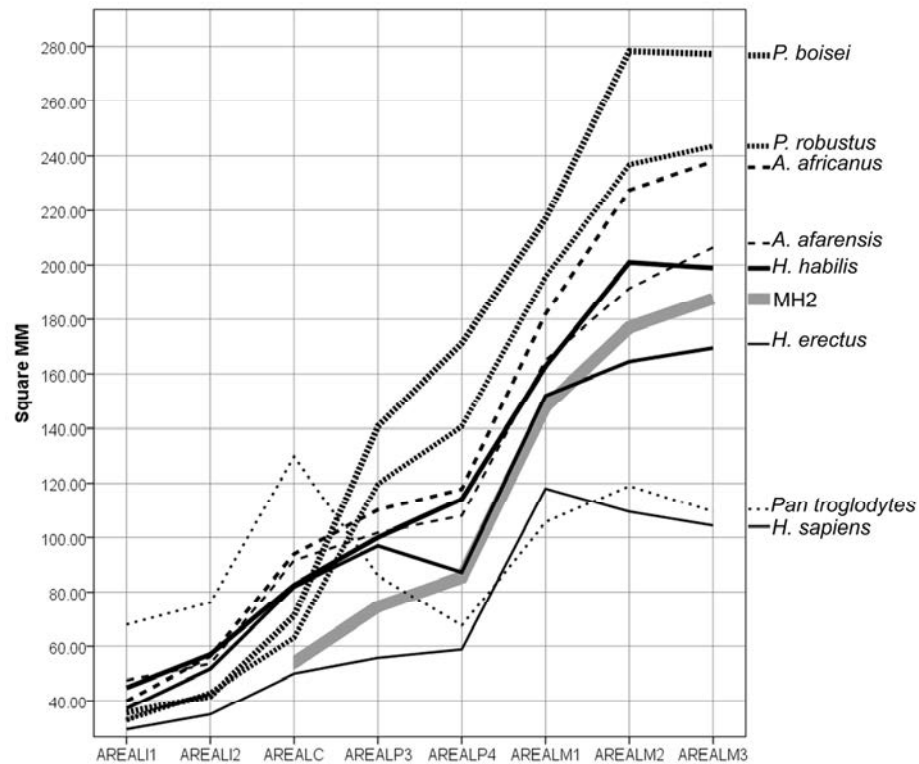


Figure 6. Line plot showing tooth-by-tooth trends in absolute occlusal surface areas (MD x BL) of the mandibular dentition in mm<sup>2</sup> by sample. Missing LI1 and LI2 MD dimensions do not permit area calculations for these teeth in MH2.  
121x97mm (300 x 300 DPI)

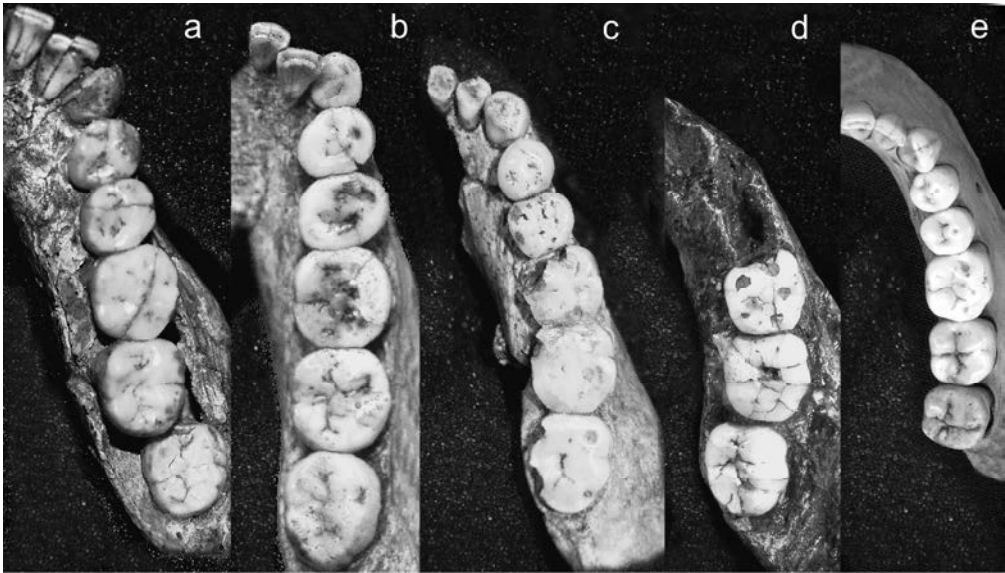


Figure 7. South African right\* mandibular dentitions from (a) *A. africanus* (STS 52), (b) *P. robustus* (SK 23), (c) *A. sediba* (MH2)\*\*, (d) *H. erectus* (SK 15), and (e) *H. sapiens* (modern), to further illustrate inter-species size variation. Some mandibles are deformed via diagenesis, but all are at same scale and positioned similarly – with LM2 buccal and lingual margins oriented vertically and LM1 mesial margins aligned horizontally. \*The more complete left SK 15 dentition was flipped to the right in the image (d). \*\*Note MH2 crown wear and damage detailed in the text. Photographs by JDI.  
254x144mm (300 x 300 DPI)

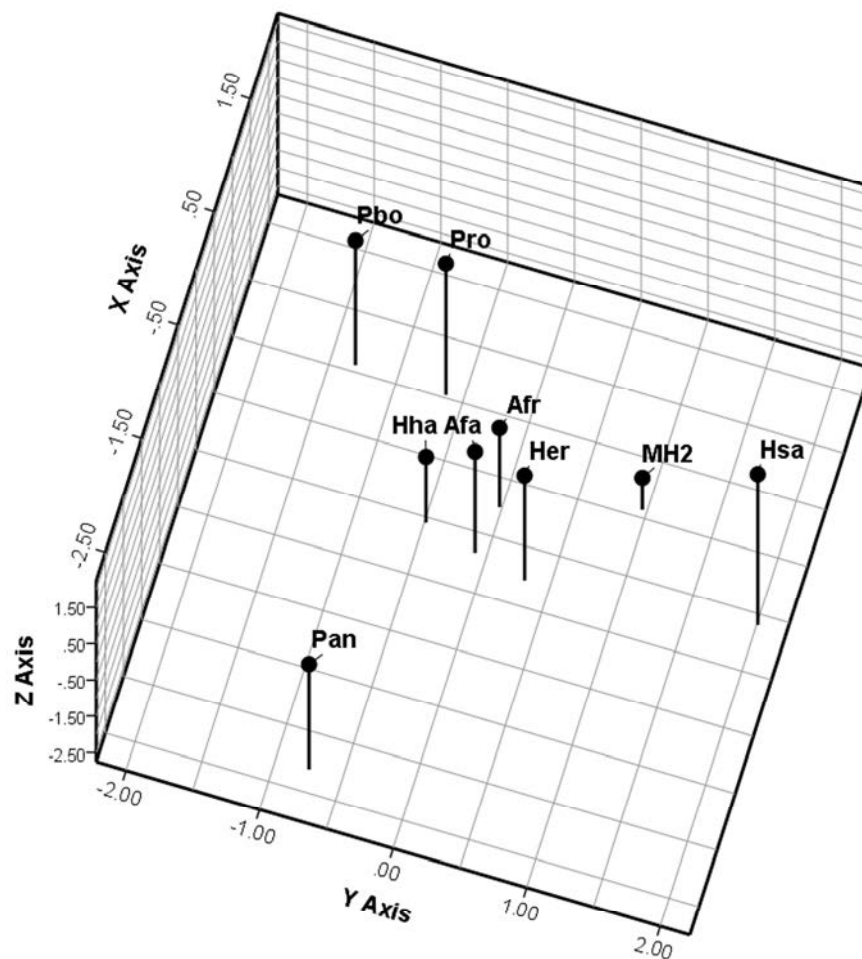


Figure 8. Three-dimensional ordination of retained principal component scores for tooth size apportionment in the mandibular dentition of *A. sediba* (MH2) and eight comparative samples. Components 1 and 2 account for 90.2% of the total variance (81.5% on X axis and 7.7% on Y axis). Component 3 provides little additional information, but its group component scores are plotted to promote comparability with other MDS figures (see text for details). Afa = *A. afarensis*, Afr = *A. africanus*, Her = *H. erectus*, Hha = *H. habilis*, Hsa = *H. sapiens*, Pan = *Pan troglodytes*, Pbo = *P. boisei*, Pro = *P. robustus*.  
158x164mm (300 x 300 DPI)

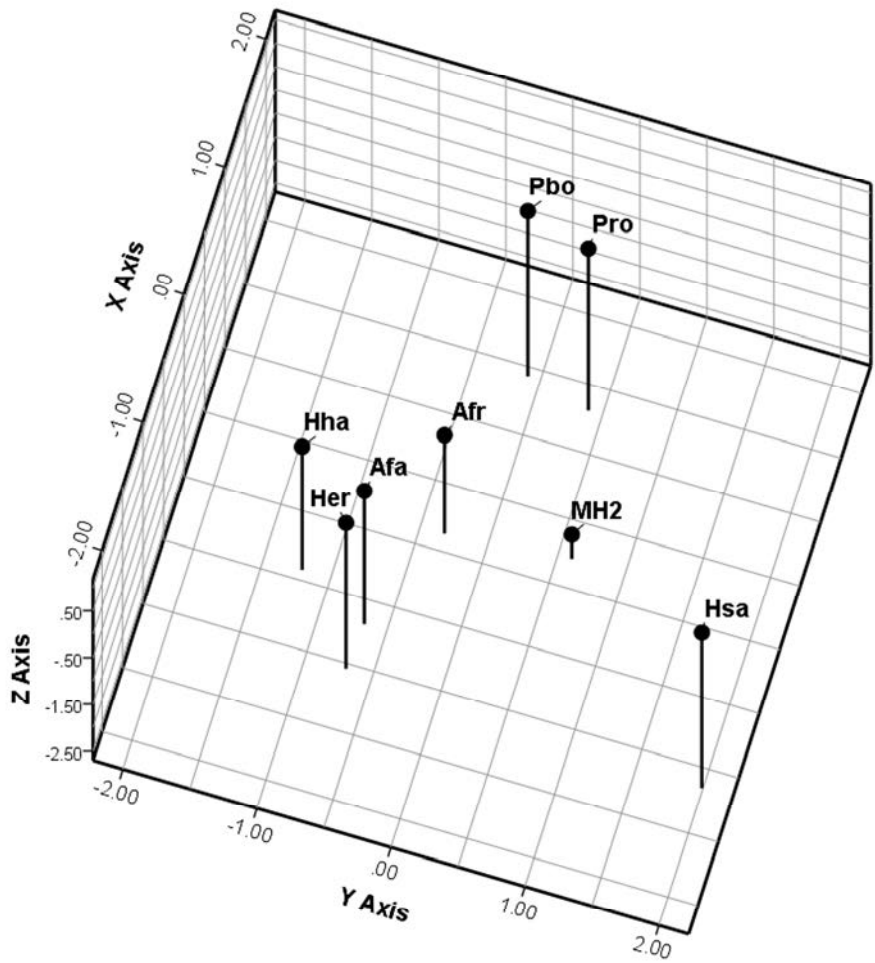


Figure 9. Three-dimensional ordination of retained principal component scores for tooth size apportionment in the mandibular dentition of *A. sediba* (MH2) and seven comparative hominin samples (i.e., excluding *Pan*). Accounts for 93.1% of the total variance (68.5% on X axis, 12.8% on Y axis, and 11.8% on Z axis. Afa = *A. afarensis*, Afr = *A. africanus*, Her = *H. erectus*, Hha = *H. habilis*, Hsa = *H. sapiens*, Pan = *Pan troglodytes*, Pbo = *P. boisei*, Pro = *P. robustus*.  
158x164mm (300 x 300 DPI)



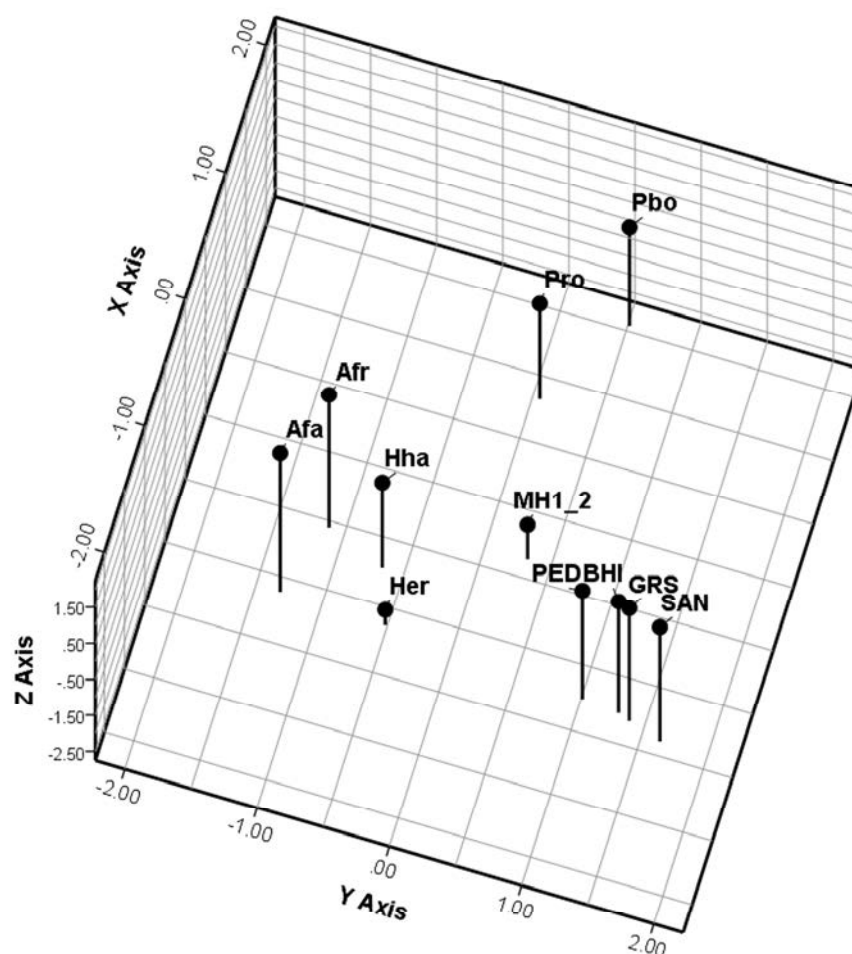


Figure 10. Three-dimensional ordination of retained principal component scores for tooth size apportionment in combined dentitions of *A. sediba* (MH1\_2) and 10 comparative samples consisting of 94 "meta-individuals" each. Accounts for 90.1% of the total variance (69.9% on X axis, 14.9% on Y axis, and 5.3% on Z axis. Afa = *A. afarensis*, Afr = *A. africanus*, Her = *H. erectus*, Hha = *H. habilis*, Pbo = *P. boisei*, Pro = *P. robustus*, BHI = modern Indian Bhils, GRS = modern Indian Garasias, PED = modern South African Pedi, SAN = modern South African San. See text for methodological details and sample compositions.  
158x164mm (300 x 300 DPI)